

**PURDUE UNIVERSITY**  
**SCHOOL OF ELECTRICAL ENGINEERING**  
**ELECTRONIC SYSTEMS RESEARCH LABORATORY**


**JOINTLY OPTIMUM WAVEFORMS AND RECEIVERS**  
**FOR CHANNELS WITH MEMORY**

by

**J. C. Hancock and E. A. Quincy**

Technical Report No. TR-EE66-7  
Supported by  
National Science Foundation  
and  
National Aeronautics and Space Administration  
Washington, D. C.

GPO PRICE \$ \_\_\_\_\_  
CFSTI PRICE(S) \$ \_\_\_\_\_  
Hard copy (HC) \$3.00  
Microfiche (MF) .75  
# 663 July 65



APRIL 1966  
LAFAYETTE, INDIANA

N66 30767

(ACCESSION NUMBER) 86  
(THRU) \_\_\_\_\_  
(PAGES) 86  
(CODE) 07  
(CATEGORY) \_\_\_\_\_  
CR-76288  
(NASA CR OR TMX OR AD NUMBER)

FACILITY FORM 602

RESEARCH GRANTS

No. NSF GP-2898, PRF 3955

and

No. NASA NSG-553, PRF 3823

JOINTLY OPTIMUM WAVEFORMS AND RECEIVERS

FOR CHANNELS WITH MEMORY

for

NATIONAL SCIENCE FOUNDATION

and

NATIONAL AERONAUTICS AND SPACE ADMINISTRATION

WASHINGTON, D.C.

by

J. C. Hancock and E. A. Quincy

School of Electrical Engineering

Purdue University

Lafayette, Indiana

## TABLE OF CONTENTS

	Page
LIST OF FIGURES . . . . .	v
ABSTRACT . . . . .	vii
CHAPTER I INTRODUCTION . . . . .	1
1.1 The Problem . . . . .	1
1.2 Literature Survey . . . . .	2
1.3 Approach and Contributions . . . . .	4
CHAPTER II GENERALIZED BAYES RECEIVER FOR CHANNELS WITH INTERSYMBOL INTERFERENCE . . . . .	7
2.1 Mathematical Model . . . . .	7
2.2 Maximum Likelihood Ratio . . . . .	10
2.3 Receiver Structure . . . . .	12
2.4 Formulation of Probability of Error . . . . .	14
CHAPTER III BAYES RECEIVER FOR ADJACENT BAUD OVERLAP, EQUI-PROBABLE, BIPOLAR SIGNALS . . . . .	18
3.1 Maximum Likelihood Ratio . . . . .	18
3.2 Receiver Structure . . . . .	19
3.3 Formulation of Probability of Error . . . . .	19
3.4 Receiver Performance and Effect of Signal Parameters . . . . .	23
CHAPTER IV WAVEFORMS WHICH MINIMIZE PROBABILITY OF ERROR FOR CHANNELS WITH INTERSYMBOL INTERFERENCE . . . . .	26
4.1 Optimization Criterion . . . . .	26
4.2 Formulation of Calculus of Variations Problem with Two Constraints . . . . .	27
4.3 Solution in Terms of Maximum Eigenvalue and Corresponding Eigenfunction of a Symmetric Integral Operator . . . . .	31
4.4 Case Study: First-Order Channel . . . . .	36
4.5 System Performance for Jointly Optimum Waveform and Receiver with First-Order Channel . . . . .	39

## TABLE OF CONTENTS (continued)

	Page
CHAPTER V OPTIMUM SIGNALS FOR EXPERIMENTAL CHANNELS BY NUMERICAL METHODS . . . . .	43
5.1 Introduction . . . . .	43
5.2 Numerical Program for Optimum Signals . . . . .	45
5.3 Experimentally Simulated Second-Order Channel . . . . .	45
5.4 Experimental Input-Output Waveforms for Experimental Second-Order Channel . . . . .	45
5.5 Performance Comparison of Optimum System for Experimental Second-Order Channel . . . . .	48
5.6 Telephone Channel-Experimental Data . . . . .	51
5.7 Computed Input-Output Optimum Waveforms for Telephone Channel . . . . .	52
5.8 Computed Rectangular Pulse Output Waveform for Telephone Channel . . . . .	52
5.9 Performance Comparison of Optimum System for Telephone Channel . . . . .	52
CHAPTER VI CONCLUSIONS . . . . .	61
6.1 Summary and Conclusions . . . . .	61
6.2 Recommendations for Further Study . . . . .	64
BIBLIOGRAPHY . . . . .	66
APPENDIX A . . . . .	69
APPENDIX B . . . . .	76
VITA . . . . .	79

## LIST OF FIGURES

Figure	Page
2-1 Binary Communication System . . . . .	7
2-2 Typical Transmitted and Received Signal Waveforms . . . . .	8
2-3 Generalized Bayes Receiver . . . . .	13
3-1 Optimum Receiver Performance for Adjacent Baud Overlap and Equi-Probable, Bipolar Signals . . . . .	24
4-1 RC Channel Output Characteristics For Optimum Signal . . . . .	40
4-2 Comparison of Jointly Optimum Transmitter and Receiver Performance for RC Channel . . . . .	41
5-1 Block Diagram of Numerical Program . . . . .	44
5-2 Experimentally Simulated Second-Order Channel . . . . .	46
5-3 Experimental RLC Channel Impulse Response . . . . .	47
5-4 Experimental Input-Output Optimum Waveforms for RLC Channel . . . . .	47
5-5 Experimental Rectangular Pulse Input-Output Waveforms for RLC Channel . . . . .	47
5-6 Experimental RLC Channel Output Characteristics for Optimum Signals . . . . .	48
5-7 Performance Comparison of Jointly Optimum Transmitter and Receiver for Experimental RLC Channel . . . . .	49
5-8 Telephone Channel Impulse Response . . . . .	53
5-9 Input Optimum Waveform for Telephone Channel . . . . .	54
5-10 Output Optimum Waveform for Telephone Channel . . . . .	55
5-11 Rectangular Pulse Input-Output Waveforms for Telephone Channel . . . . .	56

## LIST OF FIGURES (continued)

Figure	Page
5-12 Telephone Channel Output Characteristics for Optimum Signal. . . . .	57
5-13 Performance Comparison of Jointly Optimum Transmitter and Receiver for Telephone Channel . . . . .	58

## ABSTRACT

This research considers the problem of finding the jointly optimum set of transmitted waveforms and receiver structure which minimize average probability of error, where errors are due to additive noise and intersymbol interference. The channel characteristics are assumed to be known and time-invariant.

The approach used here differs from other investigations of the joint problem in that: (1) the receiver is not restricted to the linear class and (2) the performance criterion is minimum average probability of error. The memoryless, non-linear bayes receiver structure for  $M$  bauds of pulse overlap is developed. The average probability of error is also formulated. Then the channel memory is restricted to adjacent-baud overlap ( $M = 1$ ) in order to evaluate the probability of error. An equivalent criterion to minimum average probability of error is derived for signal design from the error curves. This criterion is: (1) maximize energy transferred through the channel while (2) constraining the cross-correlation energy between the head and tail of the channel output signal. The optimum signal for an arbitrary channel is given as the eigenfunction corresponding to the maximum eigenvalue of a symmetric integral operator.

A numerical algorithm is given which was used to solve the integral equation for the optimum signal when supplied sampled values of an

experimental channel impulse response. This procedure was most effectively demonstrated with experimental telephone channel data.

Experimental, optimum input-output waveforms are shown for an experimentally simulated second-order channel. Computed, optimum input-output waveforms are shown for experimental telephone channel data.

The jointly optimum transmitter and receiver performance is given for: (1) an analytic first-order channel, (2) an experimentally simulated second-order channel and (3) data representing an experimental telephone channel with quadratic delay. The performance of the jointly optimum system for practical channels, such as the telephone channel, is shown to achieve ultimate performance. That is, maximum energy is transferred by the optimum signal while the receiver eliminates the effect of intersymbol interference.



## CHAPTER I

### INTRODUCTION

#### 1.1 The Problem

This research is concerned with the problem of finding the jointly optimum set of transmitted waveforms and receiver structure which minimize average probability of error, where errors are due to additive noise and intersymbol interference. The problem of intersymbol interference or pulse overlap occurs whenever high-speed digital communications are attempted over channels with memory. One example where intersymbol interference plays a costly role is when digital data is transmitted over telephone lines<sup>20</sup>. Other examples of channels with memory are multipath channels such as ionospheric or tropospheric scatter channels. Underwater sonar channels are another case of multipath channels.

The problem of intersymbol interference on data channels has received considerable attention in recent years<sup>1,2,4,9-11,13-16,25</sup>. However, the approach used in this research differs from previous effort in that minimum probability of error is used as the system performance criterion and the receiver is not restricted to the linear class.

In this research, the channel impulse response is assumed to be known and time-invariant. For most practical channels, a reliable

measurement representing the current impulse response would be difficult to obtain since noise is always present at the receiver input. Rather than expend more energy in the sounding signal to make a reliable measurement, a more practical approach might be to employ estimation theory to determine the present impulse response given the current signalling waveform set. The problem investigated in this research under the assumption that the channel is known and time-invariant has been considered by other investigators to be non-tractable. Consequently, employing this assumption is justified especially since results obtained for this case will provide a "best performance bound" for the case where the channel is not known and only an estimate of the impulse response is available.

## 1.2 Literature Survey

Previous research on the problem of intersymbol interference can be categorized as taking one of the following approaches: (1) Signal Design to eliminate intersymbol interference or minimize its effect, (2) Receiver Design to reduce the effect of intersymbol interference and (3) Joint Transmitter and Linear Receiver Design to reduce the effect of intersymbol interference. Most of this research was restricted to Linear Receiver Design since establishing the analytic performance of non-linear receivers is usually very complicated, if not non-tractable.

Following the Signal Design approach, a recent report by Hancock and Schwarzlander<sup>1</sup> showed that signals could be obtained which maximize energy transferred out of the class which completely eliminates intersymbol interference. However, they also showed that a lower error rate could be attained by permitting the received signals to overlap and then

basing the decision only on that portion which does not overlap with the subsequent signal. This points out the fact that although signals can be found which eliminate pulse overlap at the receiver, in so doing the energy transferred through the channel is reduced, causing the error rate to increase for a fixed noise power. Gerst and Diamond<sup>2</sup> first showed that intersymbol interference can be completely eliminated by signal design for the class of lumped, linear, time-invariant networks. Chalk<sup>3</sup> derived an optimum pulse shape for minimizing adjacent channel interference and simultaneously maximizing energy transferred through the channel. The research on signal design presented in this report differs from references 4 through 7 and reference 12 since the optimization criterion used here was minimum probability of error for systems with intersymbol interference.

From the Receiver Design approach, Helstrom<sup>8</sup> proposed a non-linear bayes receiver for M bauds of intersymbol interference. However, his model was not sufficiently general to account for interference from prior transmissions and evaluation of the receiver performance was considered non-tractable. Hancock and Aein<sup>9</sup> considered using a linear correlation receiver with memory which employed prior decisions and improved performance. Gonsalves and Lob<sup>10</sup> offered a receiver with memory for the case of adjacent baud overlap. However, they could not specify the probability of error but bounds were attained. Hancock and Chang<sup>11</sup> proposed an unsupervised learning receiver structure for channels with intersymbol interference and unknown received signal waveforms. Theoretical probability of error was not given for the intersymbol interference case. Only computer simulated results were shown. Aaron

and Tufts<sup>13,15</sup> used both minimum average probability of error and minimum mean square error criteria to specify linear, time-invariant receiving filters for digital data transmission with intersymbol interference. For signal-to-noise ratios of practical interest, the optimum linear filters were found to be representable as matched filters followed by tapped delay lines. Lucky<sup>25</sup>, et.al., devised an automatic equalization scheme to reduce the distortion caused by intersymbol interference. This scheme was implemented by a tapped delay line with tap gains automatically adjusted by measurements made on test pulses.

Two reports by Tufts<sup>14</sup> and Smith<sup>16</sup> which used the Joint Transmitter and Linear Receiver approach employed a minimum mean square error criterion on pulse amplitude modulation systems. These both differ from this research in that the receiver considered here is non-linear and the performance criterion is minimum average probability of error.

### 1.3 Approach and Contributions

The approach used in this thesis to reduce the effect of intersymbol interference is joint transmitter and receiver design. That is, the jointly optimum transmitter waveforms and receiver structure are sought which will minimize average probability of error. The receiver is assumed to be memoryless, but it is not restricted to the linear class. In Chapter II, the receiver is shown to be non-linear for the general case. The results in Chapter V verify that for practical channels, adding memory to the receiver would not improve performance. However, adding memory to the non-linear receiver would be certain to make the evaluation of probability of error non-tractable.

An ideal approach to this problem would be to derive the bayes receiver structure from the maximum likelihood ratio. Then the next step would be to derive an expression for probability of error involving transmitted signal parameters. By applying variational techniques to this expression, the optimum signal would be sought which minimizes probability of error.

The actual approach used begins along the ideal route by deriving the receiver structure from the maximum likelihood ratio for a binary system with M bauds of overlap in Chapter II. Average probability of error is formulated also. Then in Chapter III, the pulse overlap is restricted to adjacent bauds in order to make the evaluation of probability of error tractable. The functional expression for performance is numerically integrated, revealing the effect of signal parameters. A criterion for signal design equivalent to minimizing probability of error, is derived from the family of curves representing performance. These curves show that the energy transferred through the channel should be maximized while simultaneously minimizing the head-tail cross-correlation of the received signal. In Chapter IV variational techniques are applied which yield the optimum signal as an eigenfunction corresponding to the maximum eigenvalue of a symmetric integral operator.

In order to demonstrate the validity of the approach used, a first-order channel is considered and the optimum signal is solved for analytically. Curves are given showing relative improvement in performance by using the jointly optimum transmitter and receiver compared with a rectangular pulse and correlation receiver. Additional contributions are given in Chapter V. A numerical method is discussed there which solves

for optimum signals when given sampled values of an experimental impulse response. A second-order channel is experimentally simulated, the optimum waveform is obtained numerically and then experimentally transmitted through the channel. A rectangular pulse is also transmitted through this channel. Both channel outputs are numerically processed to yield energy transferred and head-tail cross-correlation. Performance curves are given showing that the jointly optimum transmitter and receiver have a performance equal to that of a system without intersymbol interference. Also the optimum pulse transfers 1.61 db more energy than the rectangular pulse.

In order to demonstrate that this numerical procedure is valid for more arbitrary experimental channels than lumped parameter channels, experimental data for a telephone channel was subjected to the numerical algorithm and the optimum transmitter waveform obtained. Performance curves again showed that the jointly optimum transmitter and receiver perform as well as a system without intersymbol interference. Thus the effect of intersymbol interference was completely eliminated while the energy transfer was increased from that of a rectangular pulse by 10 db.

CHAPTER II

GENERALIZED BAYES RECEIVER FOR CHANNELS  
WITH INTERSYMBOL INTERFERENCE

2.1 Mathematical Model

Consider the binary communication system shown in Figure 2-1. One of two possible waveforms<sup>\*</sup>,  $\{s_1(t), s_2(t)\}$ , is transmitted over a specified channel having memory and impulse response  $h(t)$ . Noise,  $n(t)$ ,

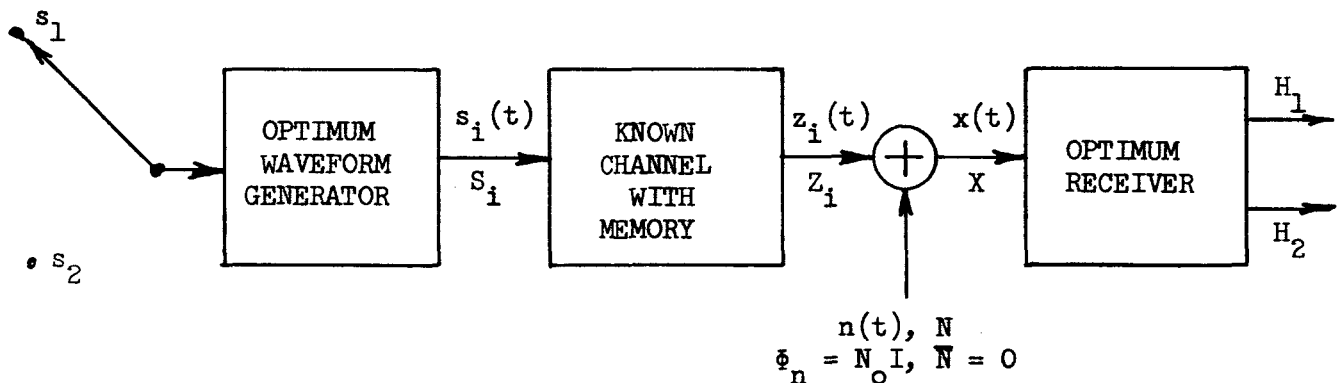


Figure 2-1. Binary Communication System

is added to the channel output,  $z(t)$ , yielding the receiver input  $x(t)$ . The receiver operates on the input,  $X$ , and then makes a hypothesis at the end of each observation interval. Either hypothesis  $H_1$  is made,

\* Throughout this research upper case letters will be used to denote matrices and either subscripted or superscripted lower case letters will be used to denote matrix elements.

announcing  $S_1$  is present or  $H_2$  is made, announcing  $S_2$  is present. These hypotheses are to be made with minimum average probability of error.

Figure 2-2 shows a typical pair of transmitted and received signal waveforms for a channel having memory. The receiver observes

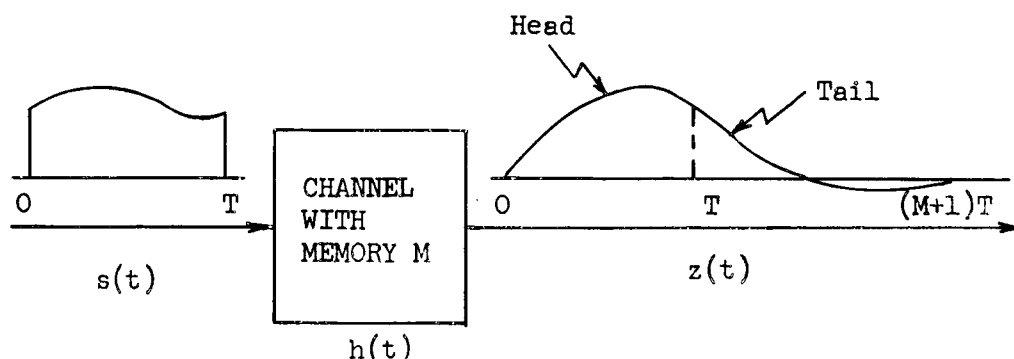


Figure 2-2. Typical Transmitted and Received Signal Waveforms

the total received signal over  $[0, (M+1)T]$ . The channel in Figure 2-2 is said to have a memory of  $M$  bauds since the output signal is stretched by a factor of at most  $M$  times the duration of the input signal. That is,  $M$  is the smallest positive integer satisfying the condition that  $z(t)$  has decayed to zero for  $t \leq (M+1)T$ .

The criterion of optimality used in jointly selecting the receiver structure and transmitted waveform is minimum average probability of error.

Let a finite set of orthonormal basis functions be chosen such that the time functions  $z(t)$  and  $x(t)$  can be represented by column vectors of the series expansion coefficients. The set of basis functions is assumed to be chosen such that the difference between the value of



inner products in integral form and vector form are arbitrarily small. The problem of selecting a finite set of basis functions to minimize a specified error is recognized as being a significant research area in recent years and will not be discussed here.

The assumptions used in the following research are listed as follows:

1. The additive noise is zero-mean, stationary, gaussian with statistically independent vector components such that  $\bar{N} = 0$  and the covariance is  $\Phi_n = N_0 I$ .  $N_0$  is the variance of each component and will be called noise power.
2. The channel impulse response is real, time-invariant, specified and exhibits  $M$  bauds of memory.
3. The signalling rate is  $1/T$  such that the output pulses overlap yielding intersymbol interference.
4. The receiver is synchronized to the transmitter starting time.
4. The receiver has zero-memory (uses only present data) with observation period  $[0, (M+1)T]$  and has available the set of possible output signal waveforms due to a single pulse of either  $s_1(t)$  or  $s_2(t)$  transmitted.

Since the signalling rate is  $1/T$ , the received signal waveforms, as shown in Figure 2-2, will have overlap. In each receiver observation time slot,  $[0, (M+1)T]$ , there are

$$r = 2^{2M} \quad (2.1)$$

possible combinations of received signal plus intersymbol interference waveforms on  $[0, (M+1)T]$  due to  $s_1(t)$  being sent on  $[0, T]$  and another

$r$  combinations if  $s_2(t)$  is sent on  $[0, T]$  making a total of  $2r$  possible waveforms plus noise that can be observed in each observation slot.

The above mathematical model of the received signal waveforms plus noise can be described as a Markov source plus gaussian noise since the observation of the signal and intersymbol interference waveform during any one time slot depends on past and future transmissions.

## 2.2 Maximum Likelihood Ratio

The bayes receiver structure can be interpreted directly from the maximum likelihood ratio for an arbitrary channel with memory  $M$ , transmitter waveform set  $\{s_1(t), s_2(t)\}$  and a priori probability set  $\{P_1, P_2\}$ . If costs are set equal, then this receiver guarantees minimum probability of error.

The likelihood ratio can be expressed as<sup>\*</sup>

$$\lambda(X) = \frac{p(X|S_1)}{p(X|S_2)} : \frac{P_2}{P_1} \quad (2.2)$$

Letting

$$K = \frac{P_2}{P_1} \quad (2.3)$$

and applying bayes rule to (2.2), the ratio can be expanded into the form

$$\lambda(X) = \frac{\sum_{j=1}^r p(X|Z_{1j}) P(Z_{1j})}{\sum_{j=1}^r p(X|Z_{2j}) P(Z_{2j})} : K \quad (2.4)$$

since specifying  $S_1$  was sent is equivalent to specifying one of the  $r$  members of the receiving set  $\{Z_{1j}\}$  was received. The total received

---

<sup>\*</sup> Throughout this research  $p$  will be used to represent probability density functions and  $P$  will denote probability.

waveform of signal and intersymbol interference plus noise is expressed in vector form as

$$X = Z_{ij} + N$$

where  $Z_{ij}$  is one of the possible  $2r$  received signals plus intersymbol interference observable on  $[0, (M+1)T]$ .

Under the additive gaussian noise assumption, the conditional densities in (2.4) can be replaced by the multivariate gaussian density

$$p(X|Z_{ij}) = \frac{e^{-\frac{1}{2}(X-Z_{ij})^T \Phi_n^{-1}(X-Z_{ij})}}{(2\pi)^{k/2} |\Phi_n|^{1/2}} \quad (2.5)$$

By substituting (2.4) into (2.3) and simplifying, the likelihood ratio can be expressed as

$$\lambda(X) = \frac{\sum_{j=1}^r c_{1j} e^{X^T \Phi_n^{-1} Z_{1j}}}{\sum_{j=1}^r c_{2j} e^{X^T \Phi_n^{-1} Z_{2j}}} : K \quad (2.6)$$

where

$$c_{ij} = P(Z_{ij}) e^{-\frac{1}{2} Z_{ij}^T \Phi_n^{-1} Z_{ij}} \quad (2.7)$$

The  $P(Z_{ij})$  are a priori probabilities and the "energy to noise" weighting coefficients are given by the exponential in (2.7). Applying the assumption that the noise samples are statistically independent, the noise covariance matrix  $\Phi_n$  reduces to

$$\Phi_n = N_o I \quad (2.8)$$

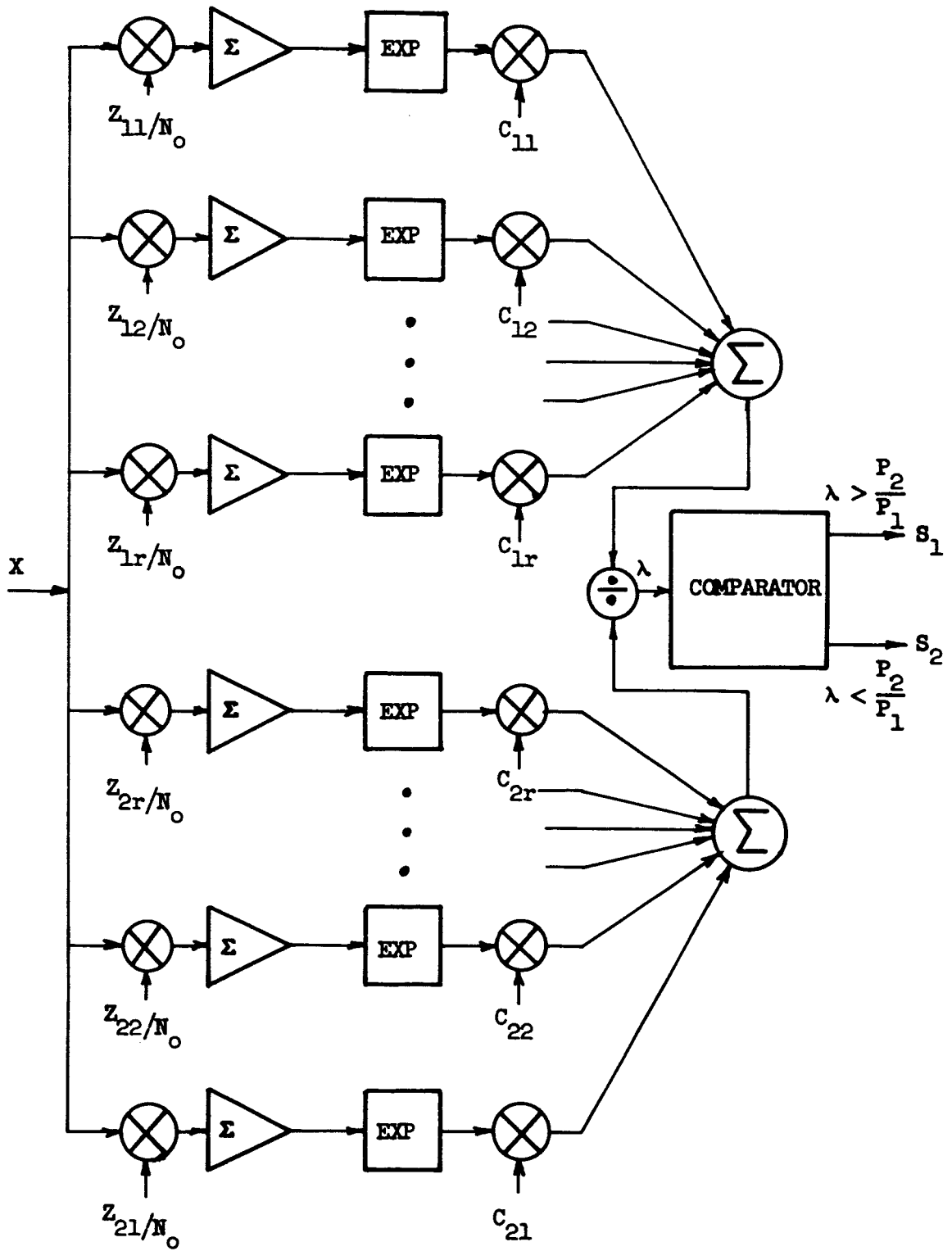
i.e., the product of noise power and the identity matrix. Applying (2.8) to (2.6), the likelihood ratio reduces to the final form of

$$\lambda(X) = \frac{\sum_{j=1}^r c_{1j} e^{\frac{1}{N_0} X^T Z_{1j}}}{\sum_{j=1}^r c_{2j} e^{\frac{1}{N_0} X^T Z_{2j}}} : K \quad (2.9)$$

where the threshold  $K$  is given by (2.2),  $r$  is given by (2.1) and  $c_{ij}$  is given by (2.7).

### 2.3 Receiver Structure

The generalized bayes receiver structure can be interpreted directly from the likelihood ratio in (2.9). Figure 2-3 gives one interpretation of (2.9) in receiver form. This receiver is not a linear correlation receiver; however, for special cases<sup>16</sup> of received signals it will reduce to that form. Equation (2.9) shows that the receiver input on  $[0, (M+1)T]$ , consisting of signal, intersymbol interference and noise, is cross-correlated with each of the  $2r$  possible waveforms of signal plus intersymbol interference. Each of these correlator outputs is exponentiated (which introduces a non-linearity) and weighted by a priori probability and "energy to noise" coefficients. Those  $r$  weighted outputs pertaining to  $s_1(t)$  being sent are summed. Similarly those  $r$  outputs pertaining to  $s_2(t)$  are summed. Then the ratio of these sums is compared to the threshold determined by the ratio of the a priori probabilities of  $s_2(t)$  and  $s_1(t)$ .



$$r = 2^M \quad (2.1) ; \quad c_{ij} = P(z_{ij}) e^{-\frac{1}{2N_0} z_{ij}^T z_{ij}} \quad (2.7)$$

Figure 2-3. Generalized Bayes Receiver

## 2.4 Formulation of Probability of Error

The average probability of error for the generalized bayes receiver above can be expressed as

$$P_e = P(\lambda < K | S_1) P_1 + P(\lambda > K | S_2) P_2 \quad (2.10)$$

where  $K$  is the threshold and the set of probabilities  $\{P_1, P_2\}$  are the a priori probabilities of the signal set  $\{S_1, S_2\}$ . Equation (2.10) can be expanded similarly to the expansion of the conditional densities in the likelihood ratio of Section 2.3, resulting in the expression

$$\begin{aligned} P_e = \sum_{\ell=1}^r [P(\lambda < K | Z_{1\ell}) P(Z_{1\ell}) P_1 \\ + P(\lambda > K | Z_{2\ell}) P(Z_{2\ell}) P_2] \end{aligned} \quad (2.11)$$

$$\begin{aligned} = \sum_{\ell=1}^r [P_1 P(Z_{1\ell}) P(\lambda_{1\ell} < K) \\ + P_2 P(Z_{2\ell}) P(\lambda_{2\ell} > K)] \end{aligned} \quad (2.12)$$

where  $\lambda_{k\ell}$  will be called a conditional likelihood ratio implying that  $Z_{k\ell}$  is given such that

$$\lambda_{k\ell} = \lambda(X | Z_{k\ell}) \quad (2.13)$$

where

$$(X | Z_{k\ell}) = Z_{k\ell} + N \quad (2.14)$$

is a gaussian random variable. From (2.9), (2.13) and (2.14) the conditional likelihood ratio can be expressed as

$$\lambda_{k\ell} = \frac{\sum_{j=1}^r c_{1j} e^{\frac{1}{N_0} (Z_{k\ell} + N)^T Z_{1j}}}{\sum_{j=1}^r c_{2j} e^{\frac{1}{N_0} (Z_{k\ell} + N)^T Z_{2j}}} : K \quad (2.15)$$

For convenience define

$$b_j = \begin{cases} c_{1j} & , \quad j = 1, 2, \dots, r \end{cases} \quad (2.16a)$$

$$b_j = \begin{cases} c_{2j} & , \quad j = r+1, r+2, \dots, 2r \end{cases} \quad (2.16b)$$

and the conditional random variables

$$w_j^{k\ell} = \begin{cases} \frac{1}{N_0} (Z_{k\ell} + N)^T Z_{1j} & , \quad j = 1, 2, \dots, r \end{cases} \quad (2.17a)$$

$$w_j^{k\ell} = \begin{cases} \frac{1}{N_0} (Z_{k\ell} + N)^T Z_{2,j-r} & , \quad j = r+1, r+2, \dots, 2r \end{cases} \quad (2.17b)$$

The set  $\{w_j^{k\ell}\}$  of  $2r$  random variables are jointly gaussian since (2.16) represents a linear operation on the gaussian noise. Employing (2.16) and (2.17) in (2.15),  $\lambda_{k\ell}$  becomes

$$\lambda_{k\ell} = \frac{\sum_{j=1}^r b_j e^{w_j^{k\ell}}}{\sum_{j=r+1}^{2r} b_j e^{w_j^{k\ell}}} : K \quad (2.18)$$

Now from (2.12) and (2.18) a typical term can be expressed as

$$P(\lambda_{1\ell} < K) = P\left( \sum_{j=1}^r b_j e^{w_j^{k\ell}} - K \sum_{j=r+1}^{2r} b_j e^{w_j^{1\ell}} < 0 \right) \quad (2.19)$$

Assuming that the set  $\{Z_{kj}\}$  of received signals plus intersymbol

interference are linearly independent then the set of jointly gaussian variables  $\{w_j^{kl}\}$  are linearly independent and the joint density is of the form

$$p(w^{kl}) = \frac{e^{-\frac{1}{2}(w^{kl} - \bar{w}^{kl})^T \Phi_W^{-1} (w^{kl} - \bar{w}^{kl})}}{(2\pi)^r |\Phi_W|^{\frac{1}{2}}} \quad (2.20)$$

From (2.17) the means are

$$\bar{w}_j^{kl} = \begin{cases} \frac{1}{N_0} Z_{kl}^T Z_{1j} & , \quad j = 1, 2, \dots, r \end{cases} \quad (2.21a)$$

$$\bar{w}_j^{kl} = \begin{cases} \frac{1}{N_0} Z_{kl}^T Z_{2,j-r} & , \quad j = r+1, r+2, \dots, 2r \end{cases} \quad (2.21b)$$

since  $\bar{N} = 0$ . The covariance matrix and inverse will be denoted by

$$\Phi_W = [\sigma_{ij}] \quad , \quad \Phi_W^{-1} = [\sigma^{ij}] \quad (2.22)$$

where

$$\sigma_{ij} = \begin{cases} \frac{1}{N_0} Z_{li}^T Z_{1j} & ; \quad i, j = 1, 2, \dots, r \end{cases} \quad (2.23a)$$

$$\sigma_{ij} = \begin{cases} \frac{1}{N_0} Z_{2,i-r}^T Z_{2,j-r} & ; \quad i, j = r+1, r+2, \dots, 2r \end{cases} \quad (2.23b)$$

$$\sigma_{ij} = \begin{cases} \frac{1}{N_0} Z_{li}^T Z_{2,j-r} & ; \quad i=1,2,\dots,r ; \quad j=r+1,r+2,\dots,2r \end{cases} \quad (2.23c)$$

Now from (2.19) and (2.20) the conditional probability of error is

$$P(\lambda_{1\ell} < K) = \iint_{R_{1\ell}} \dots \int p(w^{1\ell}) \prod_{j=1}^{2r} dw_j^{1\ell} \quad (2.24)$$

likewise

$$P(\lambda_{2\ell} > K) = \iint_{R_{2\ell}} \dots \int p(w^{2\ell}) \prod_{j=1}^{2r} dw_j^{2\ell} \quad (2.25)$$



where the regions of integration can be solved from (2.19) in terms of one of the variables as

$$R_{1l} = \left\{ w_1^{1l}, w_2^{1l}, \dots, w_{2r}^{1l} : w_{2r}^{1l} > w_{2r}^{1l*} = \ln \left( \frac{1}{Kb_{2r}} \sum_{j=1}^r b_j e^{w_j^{1l}} - \frac{1}{b_{2r}} \sum_{j=r+1}^{2r} b_j e^{w_j^{1l}} \right) \right\} \quad (2.26)$$

$$R_{2l} = \left\{ w_1^{2l}, w_2^{2l}, \dots, w_{2r}^{2l} : w_{2r}^{2l} < w_{2r}^{2l*} = \ln \left( \frac{1}{Kb_{2r}} \sum_{j=1}^r b_j e^{w_j^{2l}} - \frac{1}{b_{2r}} \sum_{j=r+1}^{2r-1} b_j e^{w_j^{2l}} \right) \right\} \quad (2.27)$$

Referring to (2.12), (2.20) and (2.25) the final form for the average probability of error for M bauds of pulse overlap is

$$P_e = \sum_{l=1}^r \left[ P_1 P(Z_{1l}) \iint_{R_{1l}} \dots \int P(w^{1l}) \prod_{j=1}^{2r} dw_j^{1l} + P_2 P(Z_{2l}) \iint_{R_{2l}} \dots \int P(w^{2l}) \prod_{j=1}^{2r} dw_j^{2l} \right] \quad (2.28)$$

Equation (2.28) shows that the probability of error is obtained from a sum of  $2r$  terms, each of which involves integration over a region of a  $2r$ -dimensional space where the boundary is specified by a transcendental equation.

## CHAPTER III

BAYES RECEIVER FOR ADJACENT BAUD OVERLAP,  
EQUI-PROBABLE, BIPOLAR SIGNALS3.1 Maximum Likelihood Ratio

The general results developed in Chapter II are applied to a special case of interest in this chapter. Since the prime objective of this research is to minimize average probability of error, the transmitted signals were chosen to be equally-probable and bipolar, i.e.,

$$P_1 = P_2, \quad S_2 = -S_1 \quad (3.1)$$

The individual signals occurring in an arbitrary sequence of transmitted signals are assumed to be statistically independent events. In order to reduce the dimension of the spaces involved in the average probability of error of (2.28) to one which might conceivably be numerically integrated, an additional assumption was placed on the channel. For the remaining research in this thesis, the memory of the channel is assumed to be  $M = 1$ , hence

$$r = 2^{2M} = 4 \quad (3.2)$$

This condition yields adjacent baud overlap only, of received signal pulses. In this case the receiver observes on  $[0, 2T]$  for signals transmitted on  $[0, T]$ .

The maximum likelihood ratio given by (2.9) reduces to

$$\lambda(X) = \frac{\sum_{j=1}^4 a_{1j} e^{\frac{1}{N_0} X^T Z_{1j}}}{\sum_{j=1}^4 a_{1j} e^{-\frac{1}{N_0} X^T Z_{1j}}} : 1 \quad (3.3)$$

where

$$a_{1j} = e^{-\frac{1}{2N_0} Z_{1j}^T Z_{1j}} = e^{-\frac{1}{2N_0} Z_{2j}^T Z_{2j}} \quad (3.4)$$

are the "energy to noise" weighting coefficients. The a priori probabilities that were involved in (2.9) have cancelled each other in the numerator and denominator of the ratio since occurrence of the transmitted signals is assumed to be statistically independent and equiprobable.

### 3.2 Receiver Structure

The receiver structure for this special case is given by Figure 2-3 where only four upper branches pertaining to  $S_1$  are required and four lower branches pertaining to  $S_2 = -S_1$  are required. In this case  $Z_{2j}$  can be replaced by  $-Z_{1j}$  for all  $j$ ,  $K$  replaced by unity and  $c_{1j}$ ,  $c_{2j}$  replaced by  $a_{1j}$  for all  $j$ .

### 3.3 Formulation of Probability of Error

For this case of only adjacent baud overlap, the number of possible received signal waveforms plus intersymbol interference on  $[0, 2T]$  is  $r = 4$  when  $S_1$  is sent on  $[0, T]$  and another four are possible when  $S_2$  is sent. The set of possible received signals plus intersymbol interference when  $S_1$  is sent is ordered as follows:

$$Z_{11} = Z + Z_t^{\ell} + Z_h^r \quad (3.5a)$$

$$Z_{12} = Z + Z_t^{\ell} - Z_h^r \quad (3.5b)$$

$$Z_{13} = Z - Z_t^{\ell} - Z_h^r \quad (3.5c)$$

$$Z_{14} = Z - Z_t^{\ell} + Z_h^r = Z_{11} - Z_{12} + Z_{13} \quad (3.5d)$$

$Z$  is the single-shot output of the channel on  $[0, 2T]$  when  $S_1$  is sent on  $[0, T]$ .  $Z_t^{\ell}$  is the tail of a  $Z$  on  $[T, 2T]$  shifted to the left by  $T$  seconds corresponding to the tail from a previous  $S_1$  transmission.  $Z_h^r$  is the head of a  $Z$  on  $[0, T]$  shifted to the right by  $T$  seconds corresponding to a future transmission of  $S_1$ . When  $S_2$  is sent, the other set of four possible received signals plus intersymbol interference will be the negative of (3.5) due to a similar ordering of subscripts and the bipolar assumption. Equation (3.5d) shows that the set of four waveforms in (3.5) is linearly dependent. Hence,  $Z_{14}$  will be replaced by a linear combination of the other three as shown in (3.5d).

From (3.3) the conditional maximum likelihood ratio can be expressed as

$$\begin{aligned} \lambda_{k\ell} &= \lambda(X|Z_{k\ell}) \\ &= \frac{\sum_{j=1}^r a_{1j} e^{w_j^{k\ell}}}{\sum_{j=1}^r a_{1j} e^{w_j^{k\ell}}} : 1 \end{aligned} \quad (3.6)$$

where

$$w_j^{k\ell} = \frac{1}{N_0} (Z_{k\ell} + N)^T Z_{1j} \quad , \quad j = 1, 2, 3, 4 \quad (3.7)$$

From (3.5d),  $w_4^{kl}$  can be replaced by a linear combination of the other three as

$$w_4^{kl} = w_1^{kl} - w_2^{kl} + w_3^{kl} \quad (3.8)$$

Substituting (3.8) in (3.6),  $\lambda_{kl}$  can be expanded as

$$\lambda_{kl} = \frac{\sum_{j=1}^3 a_{1j} e^{w_j^{kl}} + a_{14} e^{w_1^{kl} - w_2^{kl} + w_3^{kl}}}{\sum_{j=1}^3 a_{1j} e^{-w_j^{kl}} + a_{14} e^{-w_1^{kl} + w_2^{kl} - w_3^{kl}}} : 1 \quad (3.9)$$

Since the transmitted signals are equi-probable and assumed to be statistically independent, then the  $Z_{ij}$ 's will be equi-probable and the average probability of error can be expressed as a special case of (2.12) as

$$P_e = \frac{1}{8} \sum_{\ell=1}^4 \left[ P(\lambda_{1\ell} < 1) + P(\lambda_{2\ell} > 1) \right] \quad (3.10)$$

However, from the equi-probable, bipolar characteristics of the transmitted signals, the two types of error are equally likely. Hence,

(3.10) will reduce to

$$P_e = \frac{1}{4} \sum_{\ell=1}^4 P(\lambda_{1\ell} < 1) \quad (3.11)$$

From (3.9), the probabilities in (3.11) can be expressed as

$$P(\lambda_{1\ell} < 1) = P \left[ \sum_{j=1}^3 a_{1j} \left( e^{w_j^{1\ell}} - e^{-w_j^{1\ell}} \right) + a_{14} \left( e^{w_1^{1\ell} - w_2^{1\ell} + w_3^{1\ell}} - e^{-w_1^{1\ell} + w_2^{1\ell} - w_3^{1\ell}} \right) < 0 \right] \quad (3.12)$$

Solving for  $w_3^{1l}$  in terms of  $w_1^{1l}$  and  $w_2^{1l}$ , (3.12) can be rewritten as

$$P(\lambda_{1l} < 1) = P \left\{ w_3^{1l} < w_3^{1l*} = \ln \left[ -\frac{B}{2A} + \sqrt{\left(\frac{B}{2A}\right)^2 - \frac{C}{A}} \right] \right\} \quad (3.13)$$

where

$$A = a_{13} + a_{14} e^{w_1^{1l} - w_2^{1l}} \quad (3.13a)$$

$$B = a_{11} \left( e^{w_1^{1l}} - e^{-w_1^{1l}} \right) + a_{12} \left( e^{w_2^{1l}} - e^{-w_2^{1l}} \right) \quad (3.13b)$$

$$C = - \left( a_{13} + a_{14} e^{w_2^{1l} - w_1^{1l}} \right) \quad (3.13c)$$

Since the set of variables  $w_1^{1l}$ ,  $w_2^{1l}$ ,  $w_3^{1l}$  are jointly gaussian, the final form for average probability of error for the adjacent baud overlap case can be expressed as

$$P_e = \frac{1}{4} \sum_{l=1}^4 \int_{-\infty}^{\infty} \int_{-\infty}^{\infty} \int_{-\infty}^{w_3^{1l*}} p(w^{1l}) \prod_{j=1}^3 dw_j^{1l} \quad (3.14)$$

where  $w_3^{1l*}$  is given by (3.13),  $w_1^{1l}$ ,  $w_2^{1l}$ ,  $w_3^{1l}$  are given by (3.7) and

$$p(w^{1l}) = \frac{e^{-\frac{1}{2}(w^{1l} - \bar{w}^{1l})^T \Phi_W^{-1} (w^{1l} - \bar{w}^{1l})}}{(2\pi)^{3/2} |\Phi_W|^{1/2}} \quad (3.15)$$

Equation (3.14) shows that the probability of error is obtained by an integration over a region of a 3-dimensional gaussian space where the boundary of integration is described by a transcendental equation. Appendix A discusses a numerical method used to carry out the integration on the computer.

### 3.4 Receiver Performance and Effect of Signal Parameters

Figure 3-1 displays a comparison of the optimum bayes receiver performance for several pertinent values of the magnitude of  $\rho$ . Signal-to-noise ratio is defined as

$$\frac{E_o}{N_o} = \frac{\int_0^{2T} z^2(t) dt}{\sigma^2} \quad (3.16)$$

and the normalized head-tail correlation is defined by

$$\rho = \frac{\int_0^T z(t) z(t+T) dt}{E_o} \quad (3.17)$$

i.e., the ratio of channel output energy (due to a single pulse in) to the noise variance. These curves of average probability of error are the results<sup>22</sup> of numerically integrating (A.14a). Probability of error did not change as "a" -- the normalized head energy -- was varied over three typical values,  $a = 0.4, 0.5, 0.6$ . The performance for larger values of signal-to-noise ratio was not evaluated because of simultaneous underflow and overflow occurring in the same arithmetic computer statement.

Curve number 1 -- the lowest curve, is the performance of the optimum bayes receiver for orthogonal head and tail ( $\rho=0$ ). Quincy<sup>17</sup> showed that when the head and tail are orthogonal, the optimum receiver can be reduced to a linear correlation receiver. This curve also corresponds to the performance of the optimum receiver and a standard correlation receiver when no intersymbol interference is present.

Curve number 2 shows that performance of optimum receiver at

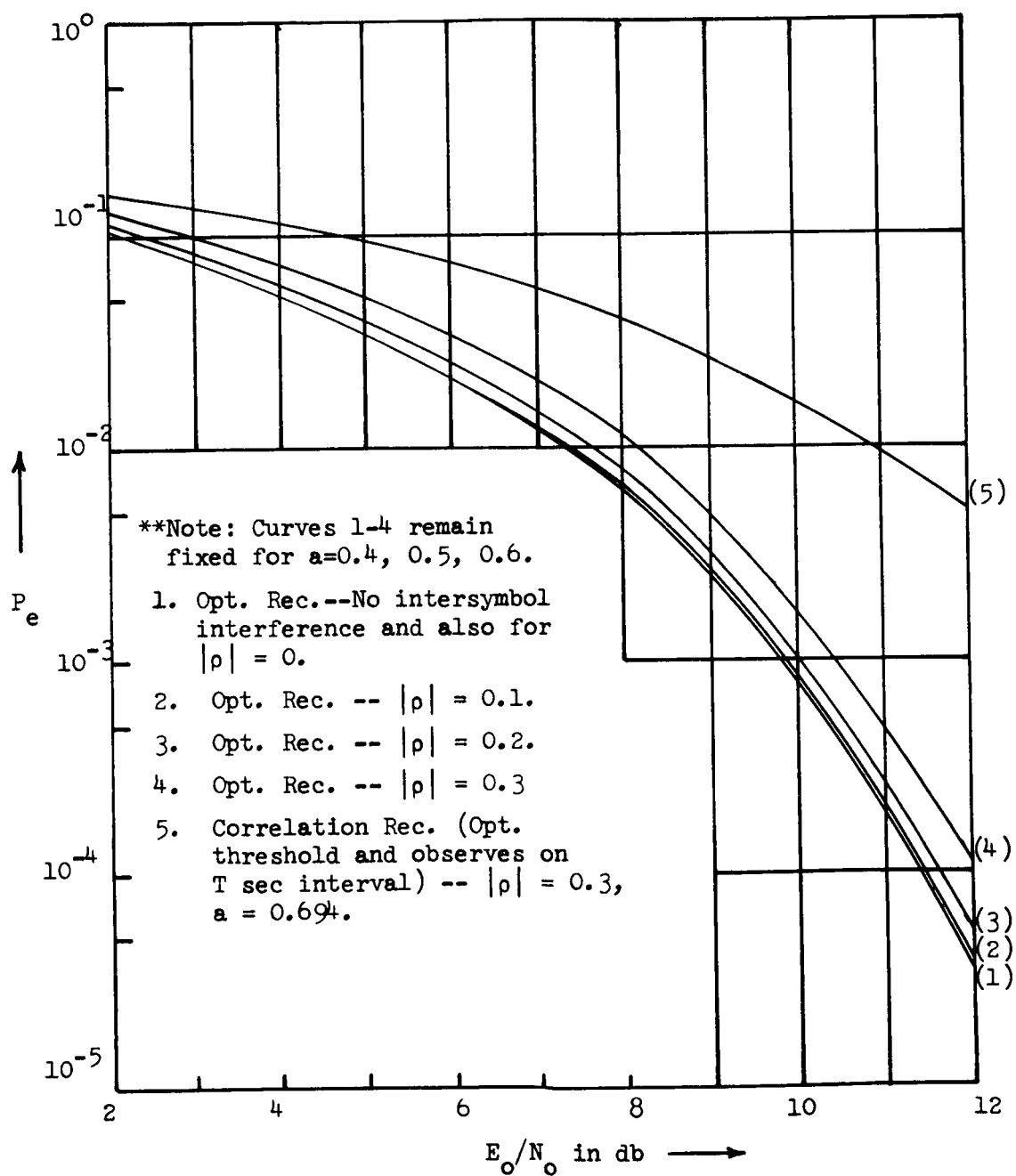


Figure 3-1. Optimum Receiver Performance for Adjacent Baud Overlap and Equi-Probable, Bipolar Signals



$E_o/N = 8\text{db}$  is degraded by less than 0.1 db for  $|\rho| = 0.1$ , compared to no intersymbol interference. Curves 3 and 4 show that probability of error increases monotonically for increasing  $|\rho|$ . For the specific channels considered in this research, signal design for maximum energy transferred produced signals with  $|\rho| < 0.3$  and in some cases  $|\rho|$  was less than 0.1.

Curve number 5 -- the top curve of Figure 3-1, represents the performance of a standard correlation receiver with the threshold optimized for intersymbol interference. The performance for this receiver is given<sup>26</sup> by

$$P_e = \frac{1}{2} \frac{1}{\sqrt{2\pi}} \int_{-\infty}^{-\sqrt{a \frac{E_o}{N_o} (1+\rho/a)}} e^{-u^2/2} du + \frac{1}{2} \frac{1}{\sqrt{2\pi}} \int_{-\infty}^{-\sqrt{a \frac{E_o}{N_o} (1-\rho/a)}} e^{-u^2/2} du \quad (3.18)$$

This receiver observes on  $[0, T]$  only over the head of the received signal. The percentage of received energy in the head for this example, was  $a = 0.694$  and the normalized head-tail cross-correlation energy was  $|\rho| = 0.3$ . At  $E_o/N = 8\text{db}$ , the performance of the standard correlation receiver is approximately 2.7 db worse than the optimum receiver, in terms of signal-to-noise ratio. This separation increases rapidly as any one of the following occurs:

1.  $E_o/N_o$  increases.
2.  $a$  decreases.
3.  $\rho$  increases.

# CHAPTER IV

## WAVEFORMS WHICH MINIMIZE PROBABILITY OF ERROR

### FOR CHANNELS WITH INTERSYMBOL INTERFERENCE

#### 4.1 Optimization Criterion

Channels with memory of  $M = 1$ , i.e., adjacent baud overlap, will be assumed in this chapter in order that an optimization criterion for selecting transmitted waveforms may be extracted from  $P_e$  -- the probability of error given in section 3.4. This probability of error was derived for the class of channels with unit memory and equally-likely, bipolar (but otherwise arbitrary) signals.

Figure 3-1 shows the effect of received signal parameters on probability of error. Since the channel impulse response is given, these channel output parameters can be related directly to the transmitted signal by the convolution integral. The two received signal parameters appearing in the performance curves of 3-1 are  $E_0$  -- the signal energy out of the channel and  $|\rho|$  -- the magnitude of the cross-correlation of the head and tail normalized to  $E_0$ . For a fixed signal-to-noise ratio,  $P_e$  is a monotonic increasing function of  $|\rho|$ . Hence,  $|\rho|$  should be reduced without significantly reducing  $E_0$ . Quincy<sup>17</sup> showed that in general,  $|\rho|$  cannot be made arbitrarily small without reducing  $E_0$ . The trade-off between  $|\rho|$  and  $E_0$  must be performed at each value of signal-to-noise ratio in order to show which is more

significant, a reduction in  $|\rho|$  or increase in  $E_o$ . Schwarzlander<sup>1</sup> showed that the reduction in energy transferred through a channel caused by specifying the output signal to be time-limited to the same base as the input signal (corresponds to a trivial case of orthogonal head and tail) while maximizing energy transferred, actually increases probability of error.

The optimization criterion set forth from the preceding discussion to select transmitter signal waveforms is the following:

1. Constrain  $E_i$ .
2. Constrain  $\rho$  or equivalently  $E_{ht} = \rho E_o$ .
3. Maximize  $E_o$ .

#### 4.2 Formulation of Calculus of Variations Problem With Two Constraints

The problem of selecting transmitted signal waveforms which are jointly optimum with the receiver structure can be formulated from the preceding section by selecting the signal which

$$\text{Max}_s \{ E_o - \lambda_1 E_i - \lambda_2 E_{ht} \} \quad (4.1)$$

i.e., select the signal which maximizes the channel output energy with the input energy constrained to  $E_i$  and the cross-correlation energy of the head and tail constrained to  $E_{ht}$ . The class of problems described by (4.1) includes the problem of maximizing energy transferred through a channel of arbitrary memory, solved by Chalk<sup>3</sup>, as a special case when  $\lambda_2 = 0$ .

A family of optimum signals can be obtained by allowing  $E_{ht}$  to vary in the solution to (4.1). This will yield a set of values

of  $E_o$  as a function of  $E_{ht}$ . The ultimate minimum probability of error signal can be obtained at each value of signal-to-noise ratio by performing a trade-off between  $E_o$  and  $E_{ht}$  on the family of curves for probability of error in Figure 3-1.

In order to take advantage of symmetry, the transmitted signal is shifted in time such that  $s(t)$  occurs on  $[-L, L]$  where

$$L = T/2 \quad (4.2)$$

Consequently the channel output  $z(t)$ , will be observed on  $[-L, 3L]$  for these physically realizable channels of unit memory. After the solution for an optimum signal is obtained,  $s(t)$  can be shifted back onto  $[0, T]$  and likewise  $z(t)$  onto  $[0, 2T]$ .

The energy out of the channel can be expressed as

$$E_o = \int_{-\infty}^{\infty} z^2(t) dt \quad (4.3a)$$

$$= \int_{-L}^{3L} z^2(t) dt \quad (4.3b)$$

where

$$z(t) = \begin{cases} \int_{-L}^t s(\tau) h(t-\tau) d\tau & , \quad -L \leq t \leq 3L \\ 0 & , \quad \text{otherwise} \end{cases} \quad (4.4)$$

In the frequency domain (4.3) becomes

$$E_o = \int_{-\infty}^{\infty} Z(f) Z^*(f) df \quad (4.5a)$$

$$= \int_{-\infty}^{\infty} [s(f) H(f)] [s^*(f) H^*(f)] df \quad (4.5b)$$

where the \* represents complex conjugate. Employing the Fourier integral, (4.4b) can be rewritten as

$$E_o = \int_{-\infty}^{\infty} \left[ \int_{-L}^L s(\tau) e^{-j\omega\tau} d\tau \right] \left[ \int_{-L}^L s(t) e^{j\omega t} dt \right] |H(f)|^2 df \quad (4.5c)$$

Assuming the order of integration is arbitrary, (4.5c) can be replaced by

$$E_o = \int_{-L}^L \int_{-L}^L s(t)s(\tau) \left[ \int_{-\infty}^{\infty} |H(f)|^2 e^{j\omega(t-\tau)} df \right] d\tau dt \quad (4.5d)$$

$$= \int_{-L}^L \int_{-L}^L s(t)s(\tau) K_1(t,\tau) d\tau dt \quad (4.5e)$$

where

$$K_1(t,\tau) = K_1^*(\tau,t) \quad (4.6a)$$

$$= \int_{-\infty}^{\infty} |H(f)|^2 e^{j\omega(t-\tau)} df \quad (4.6b)$$

is a symmetric functional and  $H(f)$  is the transfer function of the channel.

The energy into the channel is given by

$$E_i = \int_{-L}^L s^2(t) dt \quad (4.7)$$

Figure 2-2 describes the head and tail of a signal out of a channel. Head-tail cross-correlation energy is defined as

$$E_{ht} = \int_{-L}^L z(t) z(t+2L) dt \quad (4.8)$$

From (4.4) and employing the causal property of the impulse response, (4.8) can be rewritten as

$$E_{ht} = \int_{-L}^L \int_{-L}^L \int_{-L}^L s(\tau)s(x)h(t-\tau)h(t+2L-x) d\tau dx dt \quad (4.9a)$$

Interchange the dummy variables  $x$  and  $t$  in order to obtain a form similar to (4.5d). Assuming that the order of integration is arbitrary, (4.9a) can be rewritten as

$$E_{ht} = \int_{-L}^L \int_{-L}^L s(t)s(\tau) \left[ \int_{-L}^L h(x-\tau)h(x+2L-t) dx \right] d\tau dt \quad (4.9b)$$

In order to form a symmetric kernel in the final solution, (4.9b) can be expressed as one-half the sum of two integrals where the second is identical to the first except for an interchange of dummy variables  $t$  and  $\tau$ . Hence,

$$E_{ht} = \int_{-L}^L \int_{-L}^L s(t)s(\tau) \left\{ \frac{1}{2} \int_{-L}^L \left[ h(x-\tau) h(x+2L-t) + h(x-t) h(x+2L-\tau) \right] dx \right\} d\tau dt \quad (4.10a)$$

$$= \int_{-L}^L \int_{-L}^L s(t)s(\tau) K_2(t,\tau) d\tau dt \quad (4.10b)$$

where

$$K_2(t,\tau) = K_2(\tau,t) \quad (4.11a)$$

$$= \frac{1}{2} \int_{-L}^L \left[ h(x-\tau) h(x+2L-t) + h(x-t) h(x+2L-\tau) \right] dx \quad (4.11b)$$

is a symmetric functional for real  $h(t)$ . The causal properties of  $h(t)$  are emphasized for those who integrate (4.11b).

The final formulation of the variational problem with two constraints can be expressed by employing (4.5c), (4.7) and (4.10b) in (4.1), as

$$\begin{aligned} \text{Max}_s \left\{ I(s) = \int_{-L}^L \int_{-L}^L s(t)s(\tau) K_1(t,\tau) d\tau dt - \lambda_1 \int_{-L}^L s^2(t) dt \right. \\ \left. - \lambda_2 \int_{-L}^L \int_{-L}^L s(t)s(\tau) K_2(t,\tau) d\tau dt \right\} \end{aligned} \quad (4.12a)$$

By combining integrals (4.12) becomes

$$\text{Max}_s \left\{ I(s) = \int_{-L}^L \left[ \int_{-L}^L s(t)s(\tau) K(t,\tau) d\tau - \lambda_1 s^2(t) \right] dt \right\} \quad (4.12b)$$

where

$$K(t,\tau) = K(\tau,t) \quad (4.13a)$$

$$= K_1(t,\tau) - \lambda_2 K_2(t,\tau) \quad (4.13b)$$

is symmetric for real  $h(t)$ .  $K_1$  and  $K_2$  are given by (4.6b) and (4.11b), respectively.

#### 4.3 Solution in Terms of Maximum Eigenvalue and Corresponding Eigenvector of a Symmetric Integral Operator

Suppose  $s$  in (4.12b) is the actual maximizing function. Now choose any arbitrary function  $\beta$  and any constant  $\epsilon$ . By making the following substitution

$$s \rightarrow s + \epsilon\beta \quad (4.14)$$

and applying this first variation<sup>17</sup> to (4.12b), a function of  $\epsilon$  is formed for an assigned  $s$  and  $\beta$ , i.e.,

$$\begin{aligned} I(\epsilon; s, \beta) = \int_{-L}^L \left\{ \int_{-L}^L [s(t) + \epsilon\beta(t)][s(\tau) + \epsilon\beta(\tau)] K(t,\tau) d\tau \right. \\ \left. - \lambda_1 [s(t) + \epsilon\beta(t)]^2 \right\} dt \end{aligned} \quad (4.15)$$

Then a necessary condition<sup>18</sup> for a maximum is

$$\left. \frac{dI}{d\epsilon} (\epsilon; s, \beta) \right|_{\epsilon=0} = 0 \quad (4.16)$$

Applying this condition to (4.15) yields

$$\left. \frac{dI}{d\epsilon} \right|_{\epsilon=0} = \int_{-L}^L \int_{-L}^L \left\{ [s(t) + \cancel{\epsilon \beta(t)}] \beta(\tau) + [s(\tau) + \cancel{\epsilon \beta(\tau)}] \beta(t) \right\} K(t, \tau) d\tau dt - 2\lambda_1 \int_{-L}^L [s(t) + \cancel{\epsilon \beta(t)}] \beta(t) dt = 0 \quad (4.17)$$

Since  $K(t, \tau)$  is symmetric

$$\int_{-L}^L \int_{-L}^L s(t) \beta(\tau) K(t, \tau) d\tau dt = \int_{-L}^L \int_{-L}^L s(\tau) \beta(t) K(t, \tau) d\tau dt \quad (4.18)$$

and (4.16) reduces to

$$\int_{-L}^L \beta(t) \left[ \int_{-L}^L s(\tau) K(t, \tau) d\tau - \lambda_1 s(t) \right] dt = 0 \quad (4.19)$$

For an arbitrary  $\beta$ , the bracketed coefficient of  $\beta$  in (4.19) must vanish identically on the interval  $[-L, L]$ . Hence, the final form for the optimum signal which maximizes (4.1) is

$$s(t) = \frac{1}{\lambda_1} \int_{-L}^L s(\tau) K(t, \tau) d\tau, \quad -L \leq t \leq L \quad (4.20a)$$

or

$$\int_{-L}^L s(\tau) K(t, \tau) d\tau = \lambda_1 s(t), \quad -L \leq t \leq L \quad (4.20b)$$

The real, symmetric kernel of (4.20) is given by (4.6b), (4.11b) and (4.13b) as

$$K(t, \tau) = \int_{-\infty}^{\infty} |H(f)|^2 e^{j\omega(t-\tau)} df - \frac{\lambda_2}{2} \int_{-L}^L [h(x-\tau) h(x+2L-t) + h(x-t) h(x+2L-\tau)] dx \quad (4.21)$$

and

$$L = T/2 \quad (4.22)$$



where  $T$  is the length of transmitter pulse as well as the assumed length of the channel impulse response. Equation (4.20b) shows the optimum signal is given as an eigenfunction of a symmetric integral operator. Equation (4.20) is also commonly known as a Fredholm integral equation of the second kind. Several methods are available<sup>18</sup> for solving this class of equations. However, solutions in closed form can be obtained only in special cases, such as the example in section 4.4. A numerical method for solving this class of equation for an arbitrary channel is given in Appendix B.

In order to completely specify the optimum signal, a method must be determined for specifying the Lagrangian multipliers  $\lambda_1$  and  $\lambda_2$ . At least one real eigenvalue solution to (4.20b) exists<sup>18</sup> since the kernel is real, symmetric and continuous. Generally there are infinitely many<sup>18</sup> eigenvalues, each corresponding to an eigenfunction defined within an arbitrary multiplicative constant. In exceptional cases<sup>18</sup>, a given non-zero eigenvalue may correspond to at most a finite number<sup>19</sup> of linearly independent eigenfunctions. In such cases when a distinct, non-zero eigenvalue does not correspond to a unique eigenfunction, then physical reasoning must be applied to select the desired eigenfunction. Since infinitely many eigenvalue solutions to (4.20b) may exist, the problem is to determine which one will ultimately maximize (4.1). First, consider the input energy to the channel for an optimum signal, obtained by multiplying (4.20b) by  $s(t)$  and integrating over the specified interval, i.e.,

$$\lambda_1 E_i = \lambda_1 \int_{-L}^L s^2(t) dt \quad (4.23a)$$

$$= \int_{-L}^L \int_{-L}^L s(t) s(\tau) K(t, \tau) d\tau dt \quad (4.23b)$$

Secondly, consider the equivalent form of (4.1) obtained by equating (4.1) and (4.12b), i.e.,

$$\begin{aligned} E_o - \lambda_1 E_i - \lambda_2 E_{ht} &= \int_{-L}^L \int_{-L}^L s(t) s(\tau) K(t, \tau) d\tau dt \\ &\quad - \lambda_1 \int_{-L}^L s^2(t) dt \end{aligned} \quad (4.24)$$

Now, by employing (4.23) for the optimum signal, in the right hand side of (4.24), it can be set to zero and the following equation is obtained when the optimum signal is employed in (4.24), namely,

$$E_o \Big|_{s=s_{opt}} = \lambda_1 E_i + \lambda_2 E_{ht} \quad (4.25)$$

Hence, (4.25) shows that the energy out of the channel will be ultimately maximized by choosing the largest eigenvalue and corresponding eigenfunction for (4.20b).

Equations (4.20) and (4.21) show that  $\lambda_1$  is determined by the kernel which is a function of  $\lambda_2$ . Hence, for each value of  $\lambda_2$  a new maximum  $\lambda_1$  and optimum signal will be obtained. From (4.3), (4.4) and (4.20a),  $E_o$  can be calculated as a function of  $\lambda_2$  by

$$E_o = \int_{-L}^{3L} \int_{-L}^L \int_{-L}^L s(\tau) s(x) h(t-\tau) h(t-x) d\tau dx dt \quad (4.26)$$

Likewise, from (4.9a) and (4.20a),  $E_{ht}$  can be calculated as a function

of  $\lambda_2$  by

$$E_{ht} = \int_{-L}^L \int_{-L}^L \int_{-L}^L s(\tau)s(x)h(t-\tau)h(t+2L-x) d\tau dx dt \quad (4.27)$$

By normalizing  $E_o$  to  $E_i$ , the signal efficiency is defined as

$$\eta = \frac{E_o}{E_i} \quad (4.28a)$$

and

$$E_o = \eta \Big|_{E_i=1} \quad (4.28b)$$

For the special case of  $\lambda_2 = 0$ , Chalk<sup>3</sup> showed that the eigenvalue  $\lambda_1$  is identically the signal efficiency, i.e.,

$$\eta = \lambda_1 \Big|_{\lambda_2=0} \quad (4.28c)$$

The normalized head-tail cross-correlation is defined as

$$\rho = \frac{E_{ht}}{E_o} \quad (4.29)$$

For comparison purposes  $E_i$  can be assumed to be unity; then  $\lambda_2$  can be varied in the kernel of (4.20a) and a curve computed showing  $E_o$  versus  $\rho$ . From Figure 3-1 for probability of error, the final combination of  $E_o$  and  $\rho$  can be selected which ultimately minimizes probability of error at a specified signal-to-noise ratio. This combination of  $E_o$  and  $\rho$  specify the optimum signal to be transmitted at this value of signal-to-noise ratio. This procedure must be repeated for each value of signal-to-noise ratio considered. This procedure was applied in section 4.5 and Chapter V. For the specific channels considered in this research, the range of relevant values of  $\lambda_2$  are given by

$$|\lambda_2| \leq 1 \quad (4.30)$$

#### 4.4 Case Study: First-Order Channel

An RC-lowpass channel is considered in this section in order to make an analytical comparison with other research<sup>1,3</sup>. This channel is one physical interpretation of a first-order channel. The analytic form of the optimum signal is derived here and the system performance is given in section 4.5.

The impulse response is given by

$$h(t) = \begin{cases} \alpha e^{-\alpha t} & , \quad t \geq 0 \\ 0 & , \quad t < 0 \end{cases} \quad (4.31a)$$

where

$$\alpha = \frac{1}{RC} \quad (4.31b)$$

Also the transfer function is given by

$$H(f) = \frac{\alpha}{\alpha + j2\pi f} \quad (4.32)$$

Substituting (4.32) into (4.6b) and integrating yields

$$K_0(t, \tau) = \frac{\alpha}{2} e^{-\alpha|t-\tau|} , \quad -L \leq t, \quad \tau \leq L \quad (4.33)$$

Likewise substituting (4.31a) into (4.11b) and integrating yields

$$K_2(t, \tau) = \frac{\alpha e^{-4\alpha L}}{4} \left[ e^{\alpha(t-\tau)} + e^{-\alpha(t-\tau)} - 2e^{-4\alpha L} e^{\alpha(t+\tau)} \right] ,$$

$$-L \leq t, \quad \tau \leq L \quad (4.34)$$

where the kernel is

$$K(t, \tau) = K_1(t, \tau) - \lambda_2 K_2(t, \tau) \quad (4.35)$$

By substituting (4.35) into (4.20a) and expanding the integral, the following form is obtained.

$$\begin{aligned} s(t) = \frac{1}{\lambda_1} \left[ \int_{-L}^t s(\tau) K_1(t, \tau) d\tau + \int_t^L s(\tau) K_1(t, \tau) d\tau \right] \\ - \lambda_2 \int_{-L}^L s(\tau) K_2(t, \tau) d\tau \end{aligned} \quad (4.36)$$

Differentiation with respect to  $t$  will be indicated by a prime.

Now, differentiating (4.36) with respect to  $t$  twice yields

$$\begin{aligned} s''(t) = \frac{1}{\lambda_1} \left[ \int_{-L}^t s(\tau) K_1''(t, \tau) d\tau + \int_t^L s(\tau) K_1''(t, \tau) \right. \\ \left. + s(t) \left. \frac{K_1'(t, \tau)}{\tau < t} \right|_{\tau=t} - s(t) \left. \frac{K_1'(t, \tau)}{\tau > t} \right|_{\tau=t} \right. \\ \left. - \lambda_2 \int_{-L}^L s(\tau) K_2''(t, \tau) d\tau \right] \end{aligned} \quad (4.37)$$

where, from (4.33)

$$K_1''(t, \tau) = (-\alpha)^2 K_1(t, \tau), \quad \tau \leq t \quad (4.38a)$$

$$K_1''(t, \tau) = \alpha^2 K_1(t, \tau), \quad t \leq \tau \quad (4.38b)$$

and from (4.34)

$$K_2''(t, \tau) = \alpha^2 K_2(t, \tau) \quad (4.39)$$

Substituting (4.38) and (4.39) back into (4.37) leaves

$$s''(t) = \alpha^2 \left[ \frac{1}{\lambda_1} \int_{-L}^L s(\tau) K(t, \tau) d\tau - \frac{1}{\lambda_1} s(t) \right] \quad (4.40)$$

and on substituting (4.20a) yields a second-order differential equation, i.e.,

$$s''(t) + \alpha^2 \left( \frac{1}{\lambda_1} - 1 \right) s(t) = 0 \quad (4.41)$$

Since (4.41) represents a physical system, it is satisfied by the form

$$s(t) = A e^{S_1 t} + A^* e^{S_1^* t}, \quad -L \leq t \leq L \quad (4.42a)$$

where

$$S_1 = j \alpha \sqrt{\frac{1}{\lambda_1} - 1} \quad (4.42b)$$

$$S_1^* = -S_1 \quad (4.42c)$$

In order to insure a desired degree of approximation to adjacent baud overlap, at most, the channel damping factor --  $\alpha$  should be normalized to the pulse length and restricted to

$$\alpha \geq \frac{2}{T} = \frac{1}{L} \quad (4.43)$$

where  $T$  is the pulse length. Also, the signalling rate was assumed to be  $1/T$  in Chapter III. In order to evaluate system performance for unit channel memory in the next section,  $\alpha$  was assumed to be

$$\alpha = \frac{2}{T} \quad (4.44)$$

The accuracy of the assumption of unit memory can be increased by simply increasing  $\alpha$ .

The eigenvalue --  $\lambda_1$  and  $A$  can be determined by substituting (4.42a) back into the integral equation (4.20) and equating similar

terms. That is,  $A$  can be determined within a multiplicative constant. This constant will be specified by specifying a particular value of  $E_1$ .

In Appendix B, an algorithm for numerically solving the integral equation in (4.20b) is described for an arbitrary channel. Since this general numerical method was developed, it was used to solve for the maximum eigenvalue and the form of  $s(t)$  for the RC channel above. This procedure was iterated for a range of values of  $\lambda_2$ . For an arbitrary  $\lambda_2$ , the form of  $s(t)$  was a truncated half cosine wave with phase shift determined by  $\lambda_2$ . For  $\lambda_2 = 0$ , the phase shift was zero, yielding the same form that Chalk<sup>3</sup> obtained for maximizing energy transferred through an RC channel.

#### 4.5 System Performance for Jointly Optimum Waveform and Receiver with First-Order Channel

In order to determine the optimum pair of values of  $E_0$  and  $\rho$  which are attainable for a specified channel,  $\lambda_2$  was varied in (4.20a). This procedure generated the values plotted in Figure 4-1. The values in Figure 4-1 were computed numerically by a program developed for experimental channels and described in the block diagram of Figure 5-1. Figure 4-1 shows the effect on signal efficiency --  $\eta$ , of reducing  $\rho$  in optimum signals on a first-order channel. The corresponding value of  $\eta$  and  $\rho$  for a rectangular pulse of  $T$  seconds duration, into the same channel is shown in Figure 4-1 also. For this particular RC channel ( $\alpha = 2/T$ ), the optimum signal for maximum energy transfer ( $\rho$  unconstrained), is practically a rectangular pulse. Hence it transfers just slightly more energy than a rectangular pulse. Chalk<sup>3</sup> showed that in the limit as  $\alpha \rightarrow \infty$  the optimum signal for maximum energy transfer becomes

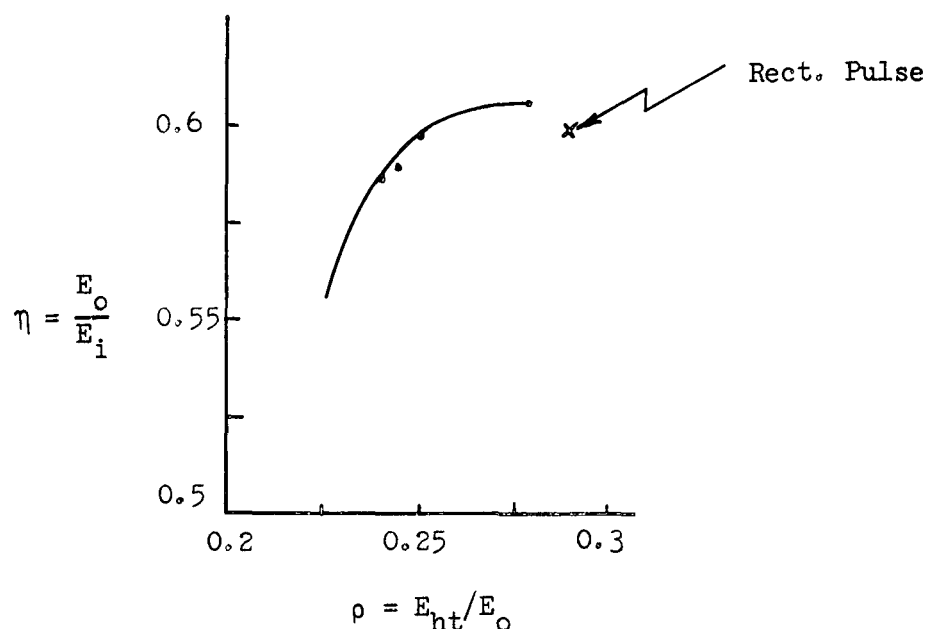


Figure 4-1. RC Channel Output Characteristics  
For Optimum Signal

rectangular. The merit of signal design becomes more apparent when  $\rho$  is constrained such as in curve number two of Figure 4-2.

Now, in order to select the optimum signal to use, a signal-to-noise ratio must be selected for the system under consideration to operate around. For comparison purposes in Figure 4-2,  $\eta_o E_i/N_o$  of 8 db was selected.  $E_i$  is the channel input energy for all systems,  $\eta_o$  is the optimum signal efficiency and  $\eta_o E_i$  is the channel output energy for the optimum signal. For this particular channel, a different selection of  $\eta_o E_i/N_o$  would not change the selection of the optimum signal significantly since  $\eta$  drops off so sharply with  $\rho$  less than 0.25. This leads to an optimum signal selection of characteristics ( $\eta_o = 0.598$ ,  $\rho = 0.250$ ). In contrast, the rectangular pulse characteristics are



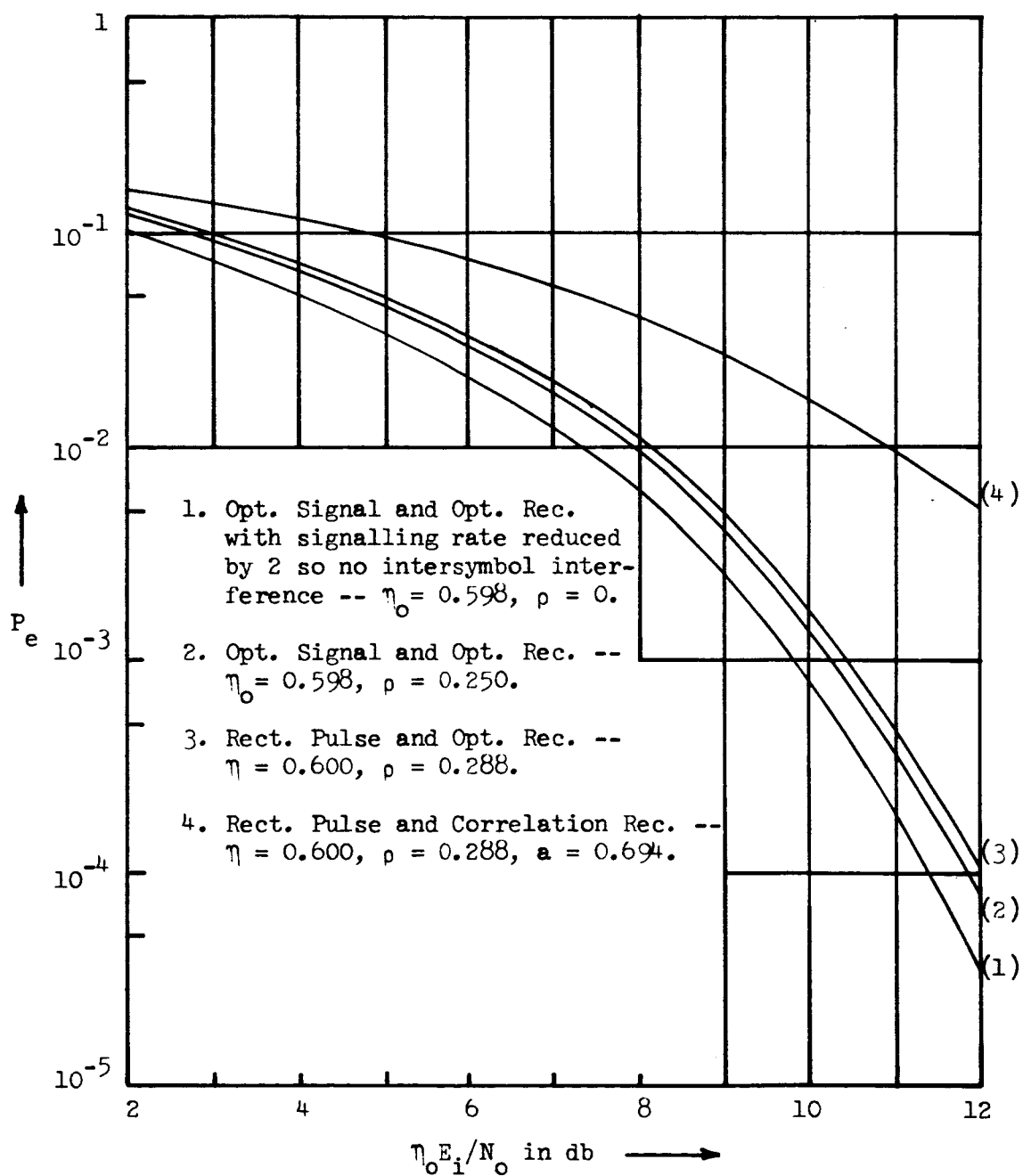


Figure 4-2. Comparison of Jointly Optimum Transmitter and Receiver Performance for RC Channel

( $\eta = 0.600$ ,  $\rho = 0.288$ ). The reduction in  $\rho$  pays off by a factor of 0.2db in signal-to-noise ratio, when used with an optimum receiver. This is demonstrated by curves two and three in Figure 4-2. Of course, if the optimum pulse were employed with a standard correlation receiver in place of a rectangular pulse, then the relative improvement would be much more significant since the standard receiver is much more sensitive to  $\rho$ . Curve four shows the system performance of a rectangular pulse employed with a standard correlation receiver whose performance is given by (3.18). Curve number one shows the optimum signal and receiver performance when the signalling rate is reduced such that no overlap of received signals occurs.

Curves one, two and four show that by employing a jointly optimum transmitter and receiver at  $\eta_0 E_i / N_0 = 8$  db, the effect of intersymbol interference has been reduced from 4 db to approximately 0.5 db in signal-to-noise ratio for an RC channel.

## CHAPTER V

## OPTIMUM SIGNALS FOR EXPERIMENTAL CHANNELS BY NUMERICAL METHODS

5.1 Introduction

This chapter considers experimental channels and offers a numerical procedure for obtaining optimum waveforms when the impulse response is available only in sampled form. Of course, if an impulse response is specified by a functional form, then it can be sampled and this method applied. The purpose of the research in this chapter is:

(1) to demonstrate that optimum signals can be obtained for experimental channels where the impulse response is specified by a set of samples, (2) to demonstrate that "optimum" signals can be generated in a piecewise approximation sense and (3) to show an improvement in performance with "optimum" signals by transmitting the "optimum" signal and a rectangular pulse through the channel, computing  $\eta$  and  $\rho$ , and then comparing probability of error curves.

In order to demonstrate that optimum signals can be obtained numerically for non-lumped-parameter, experimental channels, experimental data representing the impulse response of a telephone channel is submitted to this numerical procedure which produces the optimum signal.



## 5.2 Numerical Program for Optimum Signals

Figure 5-1 is a block diagram of major operations contained in a computer program used to solve for optimum signals when supplied an impulse response in sampled form. This program also computes channel output characteristics ( $\eta$ ,  $a$ ,  $\rho$ ) as a function of  $\lambda_2$  -- the Lagrangian multiplier representing a constraint on  $\rho$ . This makes it possible to select the ultimate optimum signal for a specific signal-to-noise ratio without making many experimental runs on the channel. This program is discussed in detail by Quincy in reference 23. The algorithm used to solve the integral equation is discussed in Appendix B.

This program can also be entered at point 5 and 7 with experimental data on channel input and output waveforms, to calculate channel output characteristics.

## 5.3 Experimentally Simulated Second-Order Channel

Figure 5-2 shows an RLC network used to simulate a lossy second-order channel of memory  $M \doteq 1$  where the transmitted signal duration is  $T = 0.001$  second. The component values were chosen to yield the underdamped impulse response shown in the photograph of Figure 5-3. The measured impulse response was scaled to account for not applying a unit area pulse in making the response measurement.

## 5.4 Experimental Input-Output Waveforms for Experimental Second-Order Channel

Figure 5-4 is a photograph of a piecewise-approximation to an optimum waveform transmitted into the RLC channel and the corresponding output waveform. This particular optimum signal was selected to generate in a piecewise approximation sense after studying the RLC channel output

characteristics in Figure 5-6. These characteristics show that an optimum signal can be obtained with  $|\rho| < 0.1$  and no significant loss in energy transferred. The experimental input-output optimum waveforms were sampled and data processed as shown in Figure 5-1. This processing yielded values of  $\eta = 0.165$  and  $\rho = -0.0748$  for the experimental optimum signal. The magnitude of  $\rho$  is sufficiently small such that performance of this signal with the optimum receiver is essentially the same as with no intersymbol interference. Performance is discussed in more detail in the next section. Figure 5-5 is a photograph of an experimental rectangular pulse into the RLC channel of Figure 5-2 and the corresponding output waveform. These were both sampled and data processed as shown in Figure 5-1. This yielded channel output characteristics of  $\eta = 0.114$  and  $\rho = -0.497$ .

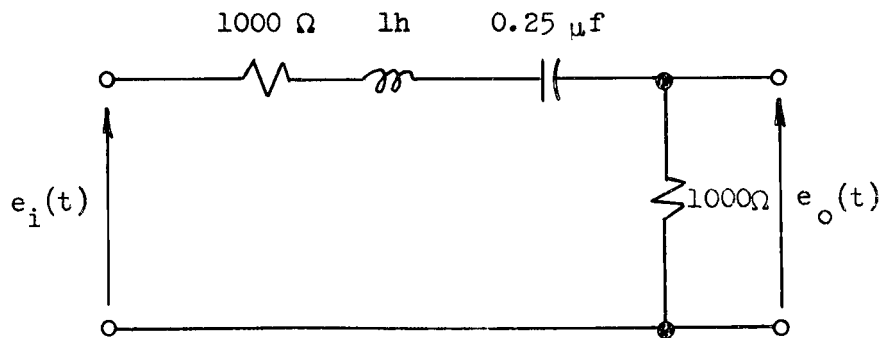


Figure 5-2. Experimentally Simulated Second-Order Channel

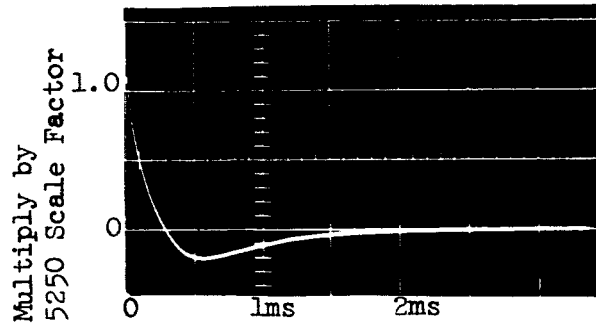


Figure 5-3. Experimental RLC Channel Impulse Response

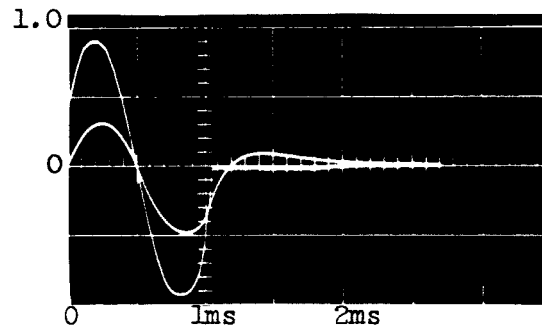


Figure 5-4. Experimental Input-Output Optimum Waveforms for RLC Channel

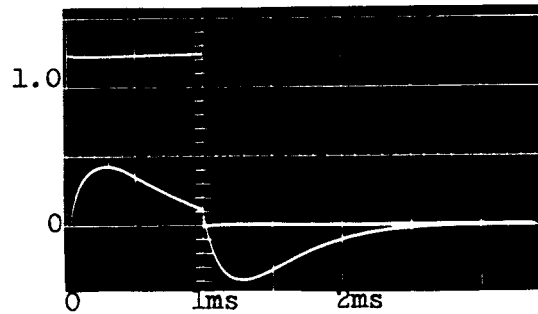


Figure 5-5. Experimental Rectangular Pulse Input-Output Waveforms for RLC Channel

### 5.5 Performance Comparison of Optimum System for Experimental Second-Order Channel

Figure 5-6 shows the output characteristics for optimum signals into the experimental RLC channel of Figure 5-2. The values of  $\eta$  and  $\rho$  were obtained numerically by supplying the computer program shown in Figure 5-1 with sampled values of the impulse response shown in the photograph of Figure 5-3. Then a range of values of  $\lambda_2$  for  $|\lambda_2| \leq 1$  were supplied to the program which computed a pair of values of  $\eta$  and  $\rho$  for each  $\lambda_2$ . This curve, relating  $\eta$  to  $\rho$ , was used to select a particular pair of values of  $\eta$  and  $\rho$  and the corresponding optimum signal to be experimentally generated in section 5.3.

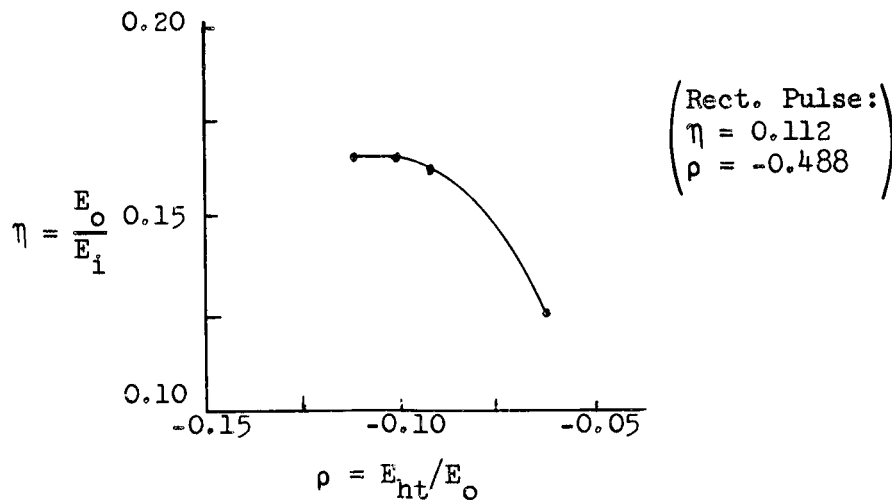


Figure 5-6. Experimental RLC Channel Output Characteristics for Optimum Signals

The values of  $\eta = 0.112$  and  $\rho = -0.448$  shown in Figure 5-6 for a rectangular pulse into the RLC channel were obtained by numerically convolving a theoretical rectangular pulse with the RLC impulse



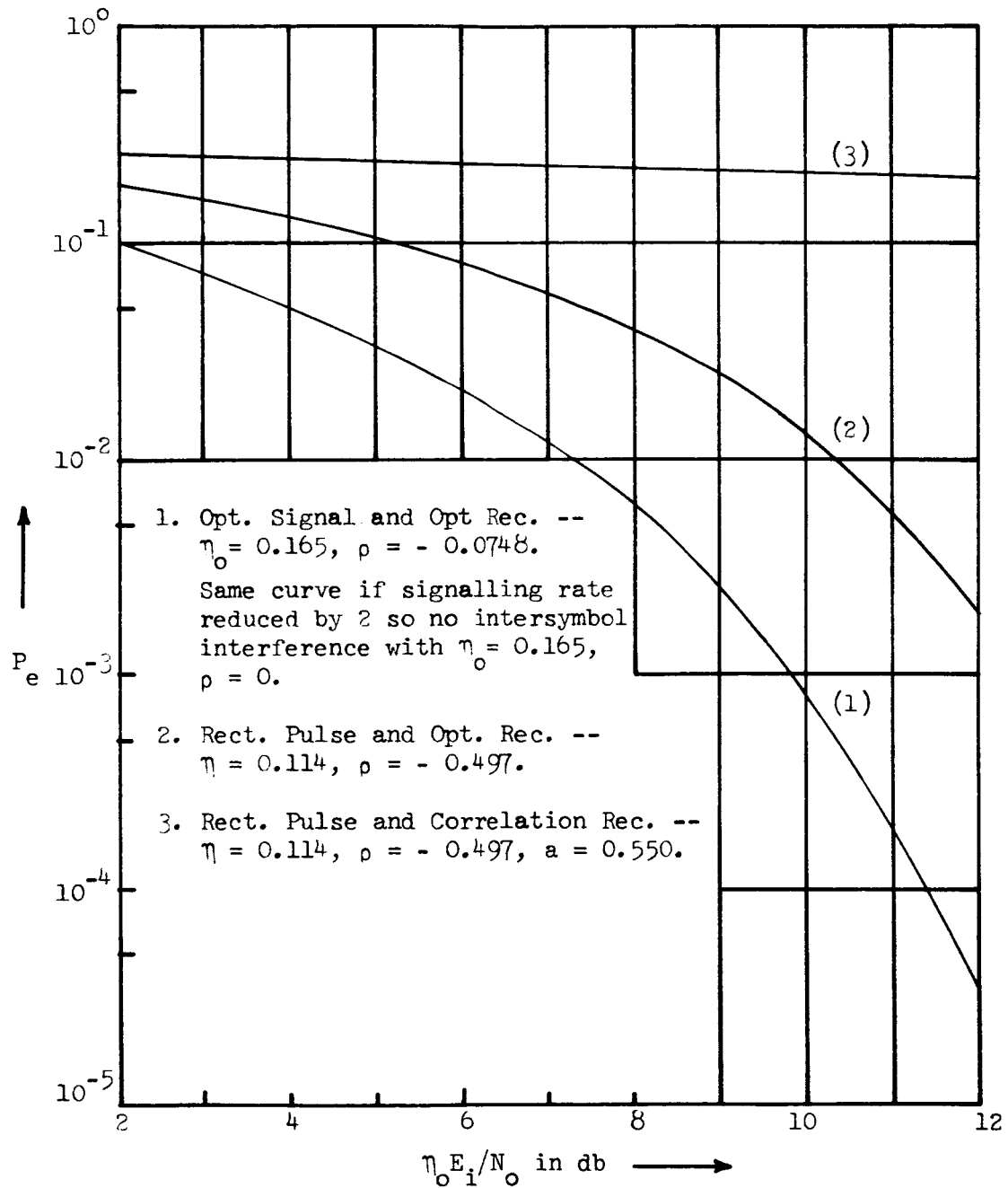


Figure 5-7. Performance Comparison of Jointly Optimum Transmitter and Receiver for Experimental RLC Channel

response and data processing this as shown in Figure 5-1.

The jointly optimum transmitter signal and optimum receiver are compared on a performance basis in Figure 5-7 with: (1) a rectangular pulse with optimum receiver and (2) rectangular pulse with standard correlation receiver. In order to compare overall communications systems, the energy into the channel is set equal for all systems. Performance is given in terms of  $\eta_o$ , input energy and noise power at the receiver input where  $\eta_o E_i$  is the optimum signal's channel output energy. The efficiency is then accounted for by horizontal translation of probability of error curves, relative to the lowest curve. Curve number one represents the jointly optimum experimental signal and optimum receiver with parameters ( $\eta_o = 0.165$ ,  $\rho = -0.0748$ ). This was determined from Figure 3-1 to be essentially the same performance as the optimum signal and optimum receiver with no intersymbol interference. This situation would occur if the signalling rate were reduced by more than 50 percent. Curve number two was obtained by an extrapolation of the curves in Figure 3-1 and represents performance of the experimental rectangular pulse with the optimum receiver for parameters ( $\eta = 0.114$ ,  $\rho = -0.497$ ). It was translated to the right by

$$10 \log (0.165/0.114) = 1.61 \text{ db}$$

to account for the loss in signal efficiency. Curve number three represents the performance of the experimental rectangular pulse with the standard correlation receiver (threshold optimized for intersymbol interference), whose performance is described by (3.18), for parameters ( $\eta = 0.114$ ,  $\rho = -0.497$ ). This curve was also translated to the right

by 1.61 db to account for loss in signal efficiency.

In comparing curves one and two, an improvement of approximately 3 db in signal-to-noise ratio is realized if the optimum signal is used in place of a rectangular pulse with the optimum receiver. In comparing curves one and three, the performance of the correlation receiver is so poor that a comparison in terms of signal-to-noise ratio cannot be made. However, an improvement in probability of error by a factor of  $2.7$  to  $7 \times 10^3$  (depending on the signal-to-noise ratio) can be realized by using the jointly optimum communication system in place of a rectangular pulse and standard correlation receiver.

Curve one represents the jointly optimum system as well as the optimum signal employed at half the signalling rate (no intersymbol interference) with a standard correlation receiver. Hence, an improvement in data rate by a factor of two can be realized with equal performance by using a jointly optimum communication system in place of using the optimum signal and standard correlation receiver with the signalling rate reduced by one-half to prevent pulse overlap. The factor of two improvement in data rate with performance improved by 1.61 db could be realized if a rectangular pulse had been employed with the correlation receiver in the preceding statement.

#### 5.6 Telephone Channel-Experimental Data

Figure 5-8 shows the impulse response of a telephone channel obtained by numerically transforming frequency domain data compiled by Alexander<sup>20</sup>, et. al. Their data was given in terms of relative attenuation and relative envelope delay. It represented an average of many

measurements made on short haul lines (4 links N carrier). The particular data used was bandpass from 130 cps to 3200 cps with quadratic envelope delay centered in the band.

The impulse response\* in Figure 5-8 drops in magnitude by a factor of 10 at approximately 3.5 milli-seconds. Since the channels considered in this research are those that yield adjacent baud overlap, the memory is said to be unity and  $T$  is taken to be 3.5 ms. Thus, an input pulse of duration  $T = 3.5$  ms will be approximately  $2T = 7$  ms duration at the channel output.

#### 5.7 Computed Input-Output Optimum Waveforms for Telephone Channel

Figures 5-9 and 5-10 show the input and output optimum waveforms respectively, for the telephone channel characterized by Figure 5-8. These were computed numerically by the program shown in Figure 5-1 and were used in computing performance shown in Figure 5-13.

#### 5.8 Computed Rectangular Pulse Output Waveform for Telephone Channel

Figure 5-11 shows an input rectangular pulse of duration 3.5 ms and the corresponding telephone channel output pulse of duration 7 ms. The output pulse was computed numerically by the program shown in Figure 5-1 and used in computing performance for Figure 5-13.

#### 5.9 Performance Comparison of Optimum System for Telephone Channel

Figure 5-12 shows the optimum signal output characteristics for the telephone channel. The curve was generated by the same method as

---

\* Note that in all computer plots, jumps are usually caused by quantized plotting rather than discontinuities in the data.

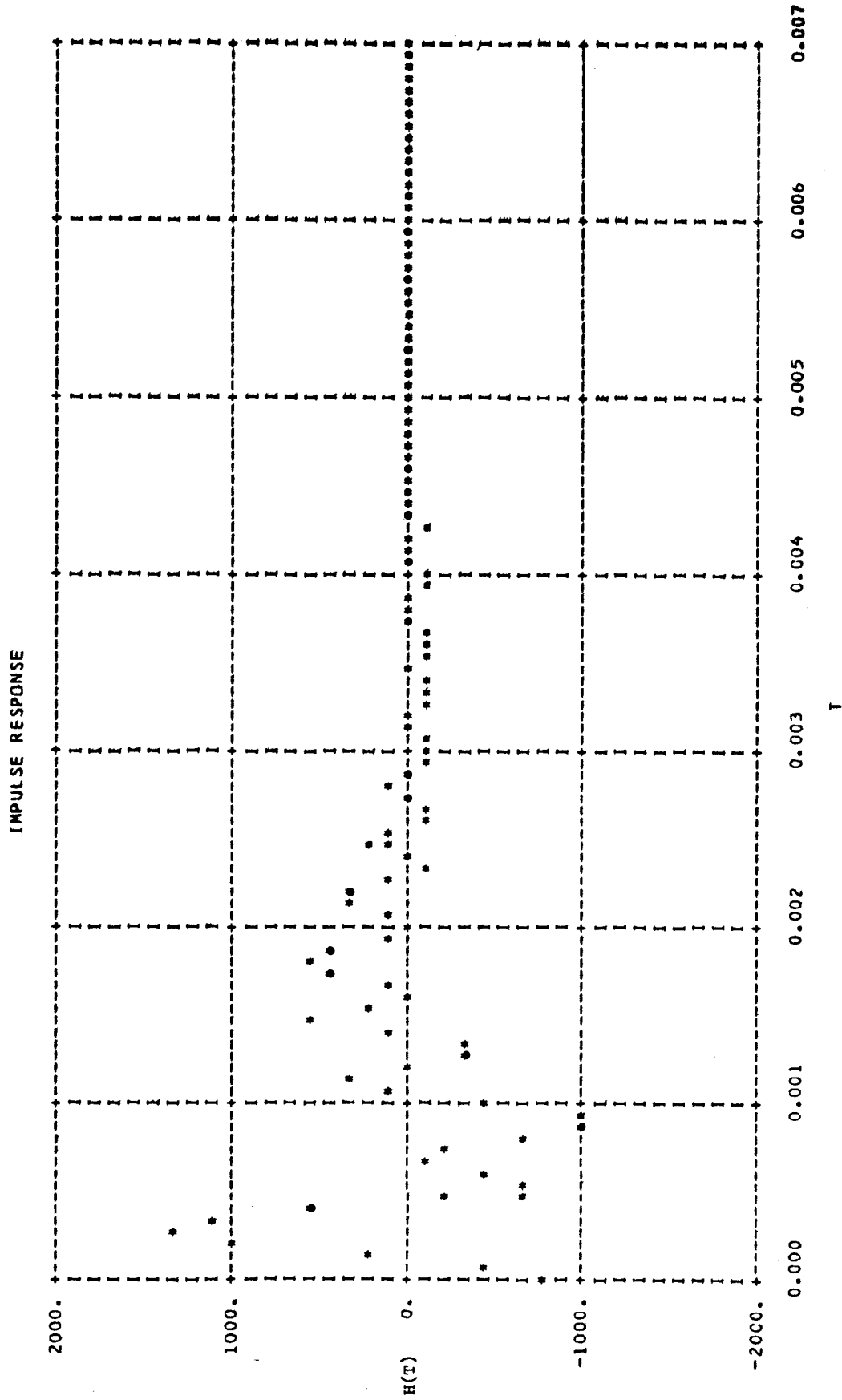


Figure 5-8. Telephone Channel Impulse Response

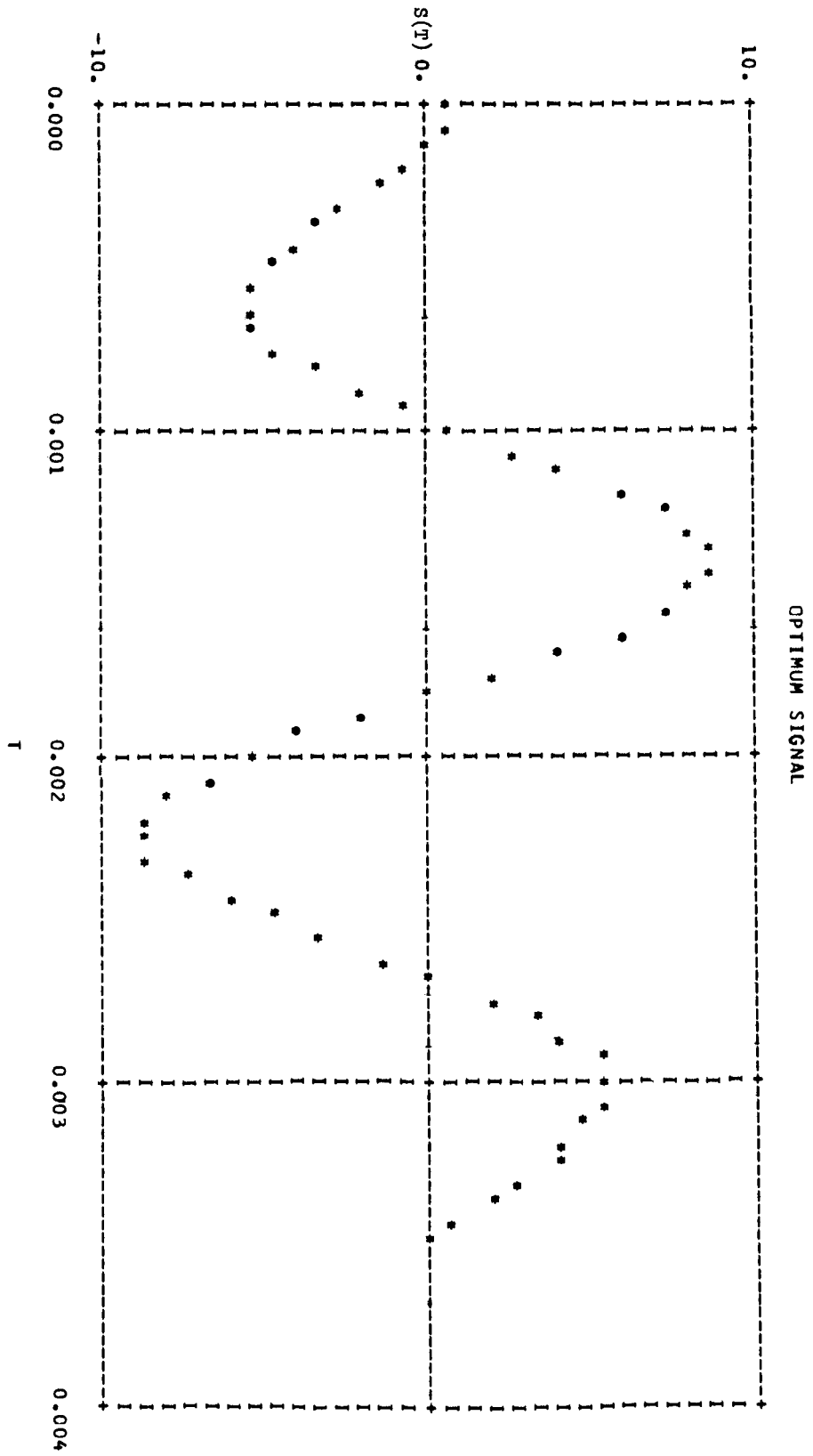


Figure 5-9. Input Optimum Waveform for Telephone Channel

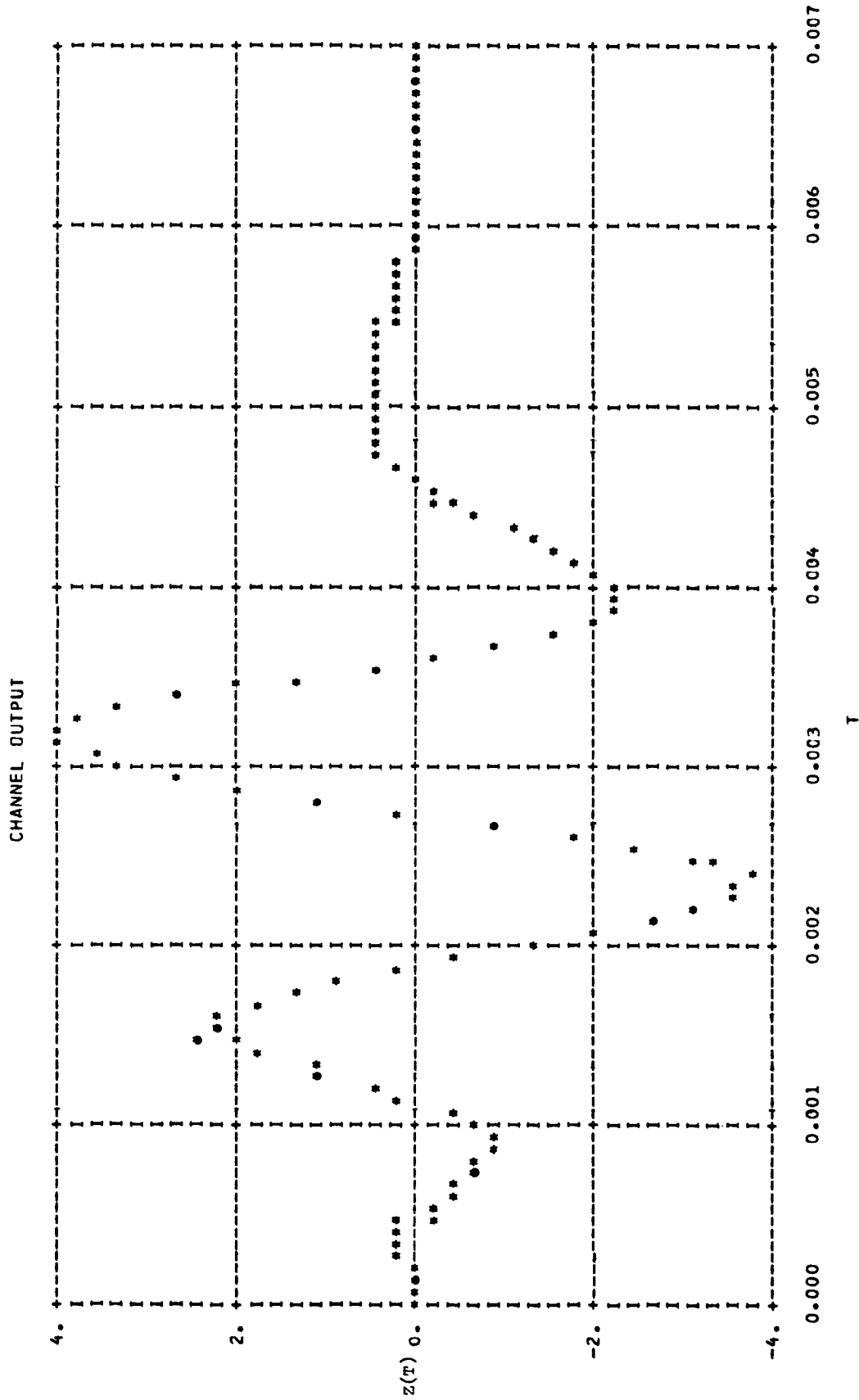


Figure 5-10. Output Optimum Waveform for Telephone Channel

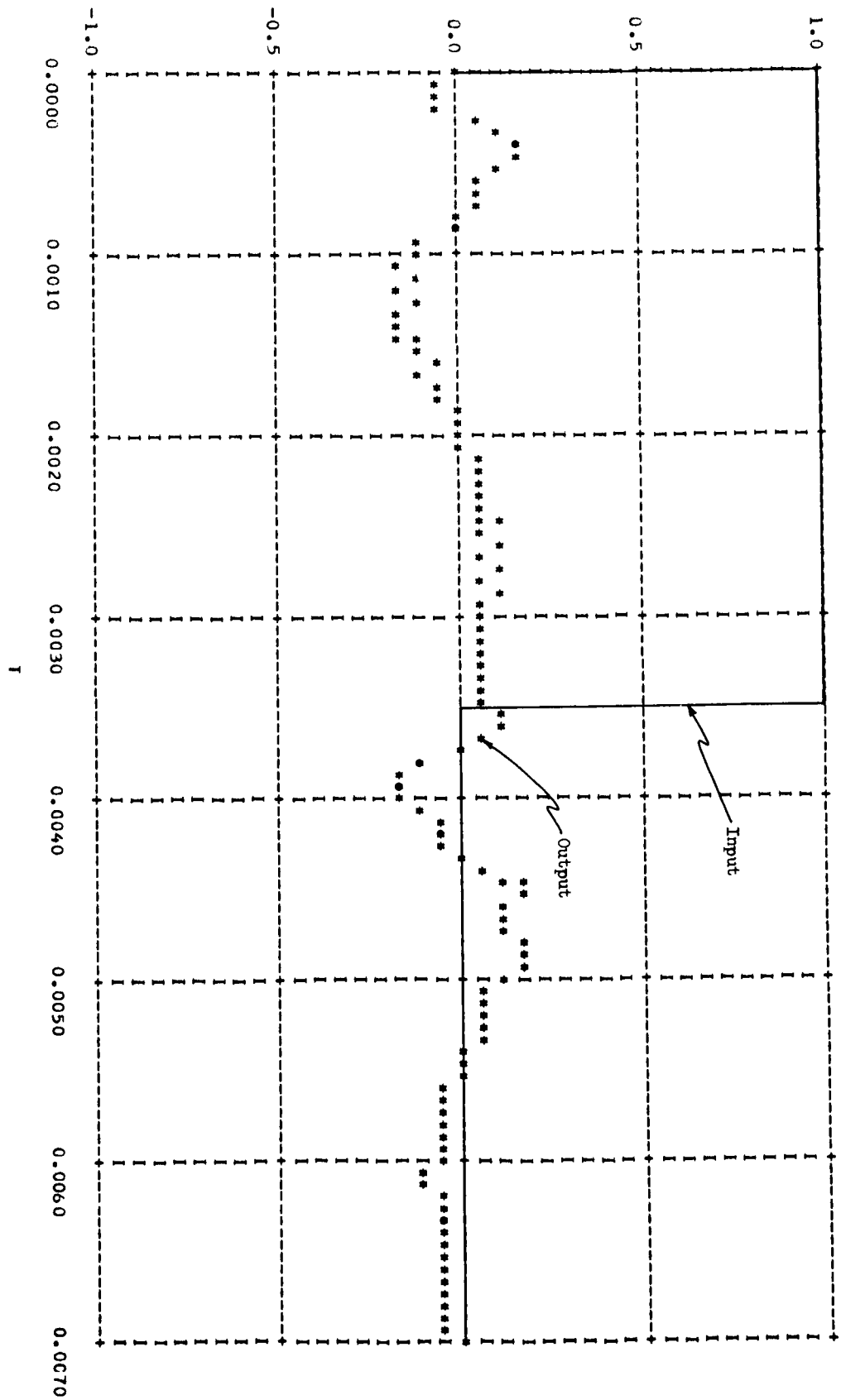


Figure 5-11. Rectangular Pulse Input-Output Waveforms for Telephone Channel



Figure 5-6. It is interesting to note from Figure 5-12, that maximum energy transfer occurs at a  $\rho$  close to zero for this practical channel.

The jointly optimum transmitter signal and optimum receiver are compared on a performance basis in Figure 5-13 with: (1) a rectangular pulse with optimum receiver, (2) rectangular pulse with standard correlation receiver and (3) rectangular pulse followed by bandpass inverse filter with standard correlation receiver. In order to compare

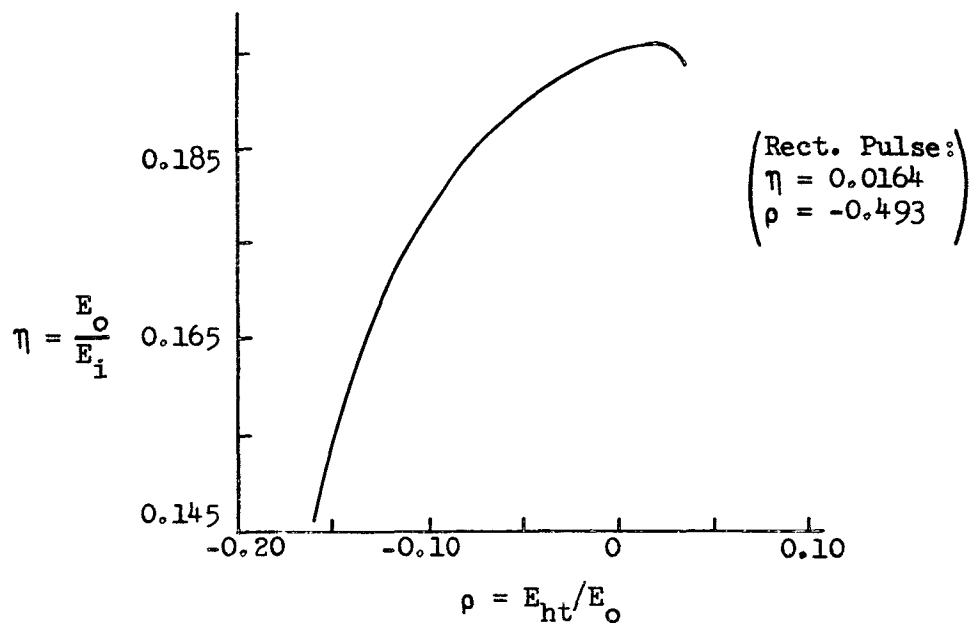


Figure 5-12. Telephone Channel Output Characteristics for Optimum Signal

overall communication systems, the energy into the channel is set equal for all systems. The signal-to-noise ratio is related to the transmitted energy as in Figure 5-7. Signal efficiency is accounted for as in Figure 5-7, by horizontal translation of receiver probability of error curves, relative to the lowest curve.

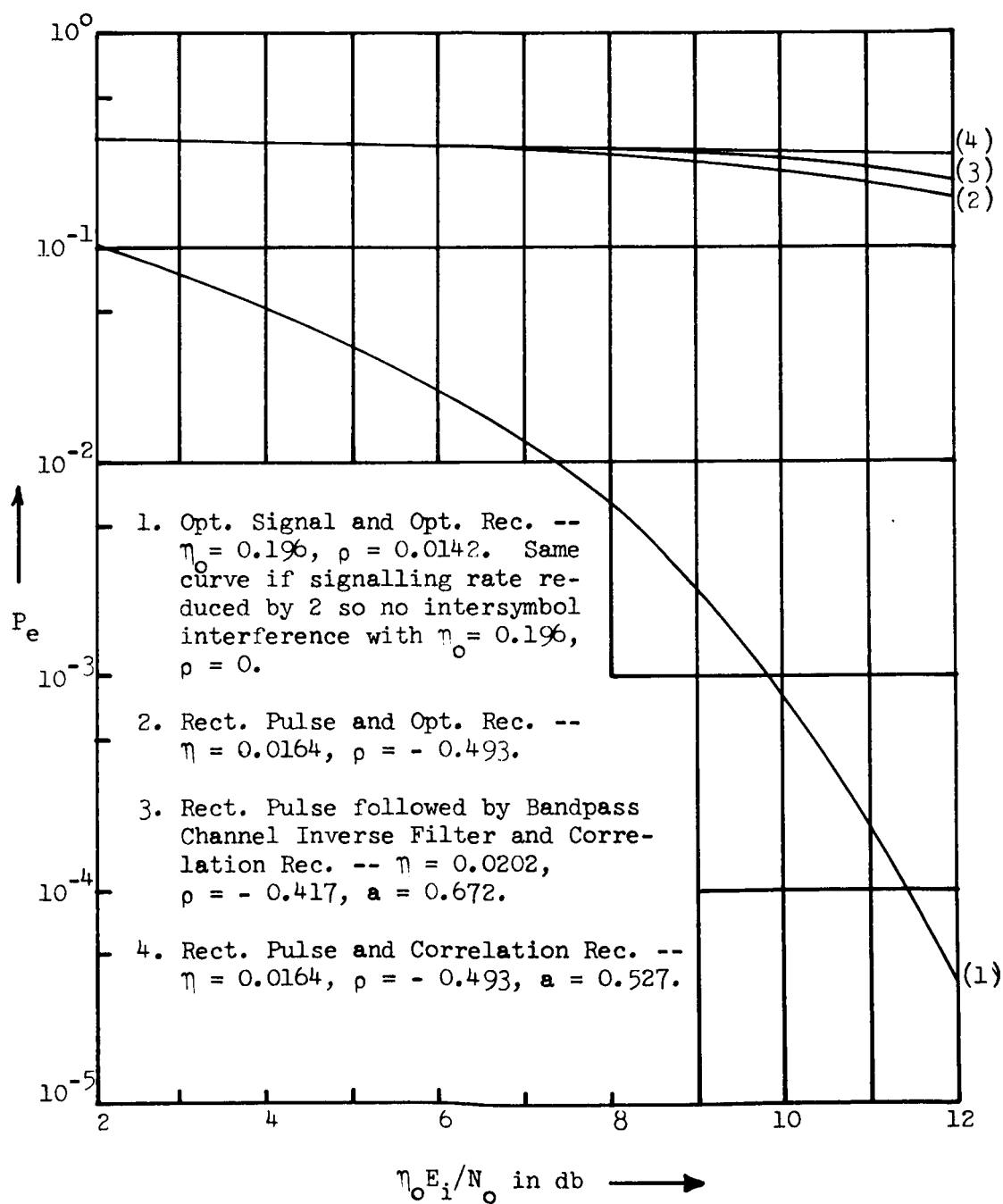


Figure 5-13. Performance Comparison of Jointly Optimum Transmitter and Receiver for Telephone Channel

Curve number one represents the jointly optimum signal and optimum receiver with parameters ( $\eta_0 = 0.196$ ,  $\rho = 0.0172$ ). Note that this signal transfers maximum energy. This was determined from Figure 3-1 to be essentially the same performance as the optimum signal and optimum receiver with no intersymbol interference which would occur if the signalling rate were reduced by at least 50 percent. Curve number two was obtained by an extrapolation of the curves in Figure 3-1. It represents performance of the experimental rectangular pulse with the optimum receiver for parameters ( $\eta = 0.0164$ ,  $\rho = -0.493$ ). The receiver performance curve was translated to the right by

$$10 \log (0.196/0.0164) = 10.8 \text{ db}$$

to account for the loss in signal efficiency, compared to the optimum signal. Curve three represents the performance of an inverse filtering system<sup>27</sup> using the standard correlation receiver whose performance is given by (3.18). A bandpass (130 to 3200 cps) inverse filter is used at the transmitter to pre-distort the rectangular pulse in an attempt to cancel the distortion or smearing characteristics of the channel which also has the same bandpass. For comparison purposes, the energy out of the inverse filter is considered to be the channel input energy. The received pulse is more nearly rectangular than the system without an inverse filter; however, there is still an overlapping tail caused by the bandpass characteristics. Considerable energy is lost from the rectangular pulse due to the bandpass characteristics. The transmitted signal parameters for this system were ( $\eta = 0.0202$ ,  $\rho = -0.417$ ,  $a = 0.672$ ) which is not significantly different from the parameters of

the rectangular pulse without an inverse filter. Curve four represents the performance of a rectangular pulse with the above standard correlation receiver (threshold optimized for intersymbol interference) for parameters ( $\eta = 0.0164$ ,  $\rho = -0.493$ ,  $a = 0.527$ ). This curve was also translated to the right by 10.8 db to account for loss in signal efficiency.

In comparing the three curves of Figure 5-13, the optimum system shows over 12 db improvement in terms of signal-to-noise ratio, compared to the sub-optimum systems. In terms of probability of error, the optimum system shows factors of improvement ranging from 3.3 to 5000 (depending on the signal-to-noise ratio) when compared to the rectangular pulse with optimum receiver. The optimum system shows even greater factors of improvement in probability of error when compared to the other two sub-optimum systems.

Since curve number one also represents the no intersymbol interference case, it shows that a factor of two improvement in data rate can be achieved by the jointly optimum system plus an improvement of 10.8 db in performance when compared to the rectangular pulse with standard correlation receiver at half the data rate (no pulse overlap case).

## CHAPTER VI

## CONCLUSIONS

6.1 Summary and Conclusions

The bayes, zero-memory receiver structure and formulation of probability of error are given for binary channels with  $M$  bauds of memory. Then the memory is restricted to unity (adjacent baud overlap) in order that the probability of error could be numerically integrated for the non-linear, optimum receiver. For signal with  $|\rho|$  as large as 0.3, the optimum receiver performance at a signal-to-noise ratio of 10 db, is within 0.6 db of the standard correlation receiver performance for no intersymbol interference. For optimum signals with  $|\rho| < 0.1$ , the optimum receiver performance at all values of signal-to-noise ratio, is essentially the same as the standard correlation receiver performance for no intersymbol interference.

An equivalent criterion to minimum average probability of error is derived for signal design from the curves for probability of error. This optimum signal criterion is: (1) maximize energy transferred through the channel while (2) constraining the cross-correlation energy between the head and tail of the channel output signal. The optimum signal for an arbitrary channel is given as the eigenfunction corresponding to the maximum eigenvalue of a symmetric integral operator.

A numerical algorithm is given which will solve the integral equation for the optimum signal when supplied sampled values of an experimental channel impulse response. This was most effectively demonstrated with experimental telephone channel data.

For practical channels such as the telephone channel, the jointly optimum transmitter and optimum receiver performance was shown to be essentially the same as performance for the same signal with a standard correlation receiver where the signalling rate is reduced by one-half to eliminate intersymbol interference. Hence, an improvement by a factor of two in data rate with equal performance, can be achieved by employing the optimum system, as compared to the optimum signal at half the signalling rate, with a standard correlation receiver. If a rectangular pulse were used with the standard correlation receiver in the preceding statement, then the optimum system would show an additional improvement in performance of 10.8 db due to the additional energy transferred by the optimum signal.

Since for practical channels the jointly optimum system achieves ultimate performance, adding memory to the receiver would be of no benefit. Consequently, the validity of zero-memory restriction used here is demonstrated.

When considering practical channels such as the telephone channel, where the optimum signal is oscillatory in nature,  $|\rho|$  can be reduced significantly without significantly reducing the energy transferred. Consequently, the optimum signal is very similar to Chalk's<sup>3</sup> signal which maximizes energy transferred -- except for primarily a phase shift which reduces  $|\rho|$ . Also, Chalk<sup>3</sup> showed that  $\eta$  for his signal

( $\lambda_2 = 0$ ) is given by the maximum eigenvalue of the integral equation representing his signal. Consequently, this eigenvalue can be used as the least upper bound on  $\eta$  for other values of  $\lambda_2$ .

The jointly optimum transmitter and optimum receiver developed in this research, possess an advantage over systems employing signals which eliminate intersymbol interference and consequently do not transfer maximum energy. In this research the channel output signal is allowed to overlap, keeping the energy transferred within 0.1 db of the maximum. However, for practical channels,  $|\rho|$  is made sufficiently small to eliminate the effect of intersymbol interference.

Since the formulation of the optimum signal does not restrict the channel memory when  $\lambda_2 = 0$ , the numerical methods employed here can be used to design signals for maximum energy transfer in other systems with arbitrary memory channels.

For practical channels and the jointly optimum transmitter and receiver,  $|\rho|$  is usually quite small (less than 0.1). Consequently, in a practical situation a trade-off might be desired between receiver complexity and system performance. If the signals are designed for  $\rho = 0$  (orthogonal head-tail), then the optimum receiver reduces from a four-branch non-linear receiver to a two-branch linear correlation receiver with observation period  $[0, 2T]$ . In general, forcing  $\rho \rightarrow 0$  can only be done at the expense of less energy transferred through the channel. Another possibility is using the optimum signal with small  $|\rho|$  in conjunction with a two-branch linear correlation receiver having observation period  $[0, 2T]$  and parameters optimized for intersymbol interference. In general, receiver performance may have to be sacrificed

for receiver simplicity. However, for the telephone channel maximum energy transfer signals exhibited  $|p|$  sufficiently close to zero such that a two-branch linear correlation receiver could be employed with the optimum signal at no significant reduction in system performance.

Performance comparisons of the optimum receiver and jointly optimum system were made with other sub-optimum systems in order to provide a feeling for the range of improvement attainable with the optimum systems. No attempt was made to find the best sub-optimum system, out of the multitude which exist, with which to compare the optimum systems. However, it should be noted that the systems presented in this research have the best theoretical performance of any systems employing the assumption used here.

## 6.2. Recommendations for Further Study

Throughout this research the channels were assumed to be known and time-invariant. A natural evolution of this work would be to consider unknown channels where the impulse response is not specified and must be determined by the system. An adaptive system with a feed-back channel should be considered. An estimation procedure could be employed at the receiver to "learn" the impulse response from the received signal plus noise, given a priori knowledge of the transmitted signal waveform. This information could then be fed back to the transmitter to up-date the optimum signal.

The next problem to be considered is the time-variant channel and then the combined problem of unknown and time-variant channel. Finally, the random, time-variant channel should be investigated.



Another major assumption employed in the latter part of this research is that the channel memory is restricted to adjacent-baud overlap. Possibly this work could be extended to  $M > 1$ . However, establishing performance for  $M = 1$  was extremely difficult and for  $M > 1$  the problem would surely be formidable if a bayes receiver is employed.

Another possible extension of this problem would be to consider  $m$ -ary signalling instead of the binary signalling used throughout this research.

## BIBLIOGRAPHY

## BIBLIOGRAPHY

1. Schwarzlander, H. and Hancock, J. C., "Signal Optimization for Digital Communication Over Channels with Memory," IEEE Symposium on Signal Transmission and Processing, pp. 56-61, Columbia University, New York, N. Y., May 1965.
2. Gerst, I. and Diamond, J., "The Elimination of Intersymbol Interference by Input Sampling Shaping," Proceedings IRE Vol. 49, p. 1195, July 1961.
3. Chalk, J., "The Optimum Pulse-Shape for Pulse Communication," Proceedings IEEE Vol. 97, Part III: 88-92, Savoy Place, London W.C. 2, England, March 1950.
4. Saltzberg, B. R. and Kurz, L., A Note on M-ary Signalling in the Presence of Additive Intersymbol Interference and Noise, Technical Report No. 400-97, AFCRL-64-656, Department of Electrical Engineering, New York University, University Heights, New York, N. Y., 1961.
5. Campbell, J. B. and Reis, F. B., Design of Input Waveforms to Yield Time-Limited Orthogonal Outputs, Scientific Report No. 3, Northeastern University, Boston, Mass., AD 411 224, March 1963.
6. Middleton, D., An Introduction to Statistical Communication Theory, Chapter 23, McGraw-Hill Book Co., Inc., New York, N. Y., 1961.
7. Lerner, R. M., Lectures on Communications System Theory, Baghdady ed., Chapters 8 and 11, McGraw-Hill Book Co., Inc., New York, N. Y., 1961.
8. Helstrom, C. W., Statistical Theory of Signal Detection, Chapter 4, Pergamon Press, Oxford, 1961.
9. Aein, J. M. and Hancock, J. C., "Reducing the Effects of Intersymbol Interference," IEEE-PGIT, Vol. IT-9: 167-175, July 1963.
10. Gonsalves, R. A. and Lob, W. H., Maximum-Likelihood Detection in a Binary Channel with Memory, Scientific Report No. 4, AFCRL-63-313, Northeastern University, Boston, Mass., July 1963.

11. Hancock, J. C. and Chang, R. W., On Reception of Signals For Channels Having Memory, Technical Report No. TR-EE65-19, School of Electrical Engineering, Purdue University, Lafayette, Indiana, October 1965. (To be published in IEEE-PGIT, October 1966.)
12. Tufts, D. W. and Shnidman, D. A., "Optimum Waveforms Subject to Both Energy and Peak-Value Constraints," Proc. of IEEE, Vol. 52, No. 9: 1002-1007, September 1964.
13. Aaron, M. R. and Tufts, D. W., "Intersymbol Interference and the Estimation of Digital Message Sequences, Presented at the International Conference on Microwaves, Circuit Theory, and Information Theory, Tokyo, Japan, September 1964, of. IEEE Trans. on Information Theory, Vol. IT-10, Abstracts Sec.: 393, October 1964.
14. Tufts, D. W., "Nyquist's Problem - The Joint Optimization of Transmitter and Receiver in Pulse Amplitude Modulation," Proc. of IEEE: 248-259, March 1965.
15. Aaron, M. R. and Tufts, D. W., "Intersymbol Interference and Error Probability," IEEE-PGIT, Vol. IT-12: 26-35, January 1966.
16. Smith, J. W., "The Joint Optimization of Transmitted Signal and Receiving Filter for Data Transmission Systems," BSTJ, Vol. XLIV, No. 10: 2363-2393, December 1965.
17. Quincy, E. A., Thesis Progress Report (To J. C. Hancock), School of Electrical Engineering, Purdue University, Lafayette, Indiana, October 1965.
18. Hildebrand, F. B., Methods of Applied Mathematics, Prentice-Hall, Inc., Englewood Cliffs, N. J., 1952.
19. Indritz, J., Methods in Analysis, The Macmillan Co., New York, N. Y., 1963.
20. Alexander, A. A., Gryb, R. M. and Nast, D. W., "Capabilities of the Telephone Network for Data Transmission," BSTJ, Vol. XXXIX, No. 3: 431-475, May 1960.
21. McCormick, J. M. and Salvadori, M. G., Numerical Methods in Fortran, Prentice-Hall, Inc., Englewood Cliffs, N. Y., 1964.
22. Quincy, E. A., Intra-Departmental Memorandum No. 1, (To J. C. Hancock) School of Electrical Engineering, Purdue University, Lafayette, Indiana, April 1966.

23. Quincy, E. A., Intra-Departmental Memorandum No. 2, (To J. C. Hancock) School of Electrical Engineering, Purdue University, Lafayette, Indiana, April 1966.
24. Mood, A. F., Introduction to the Theory of Statistics, McGraw-Hill Book Co., Inc., New York, N. Y., 1950.
25. Lucky, R. W., et. al., "Automatic Equalization for Digital Communication," Proc. of IEEE, pp. 96-97, January 1965.
26. Quincy, E. A., Ph.D. Thesis Proposal (To J. C. Hancock), School of Electrical Engineering, Purdue University, Lafayette, Indiana, March 1965.
27. Schreiner, K. E., et. al., "Automatic Distortion Correction for Efficient Pulse Transmission," IBM Journal, pp. 20-30, January 1965.

## APPENDICES

## APPENDIX A

Equation (3.14), which expresses the average probability of error for adjacent baud overlap, is expanded in this appendix to a form amenable to numerical integration. Equation (3.14) is transformed such that the first integration appears as the error function. Then the remaining two definite integrations can be performed by any integration algorithm such as Simpson's one-third rule.

Transforming the gaussian variables in (3.14) to zero-mean variables yields

$$y_j^{1\ell} = w_j^{1\ell} - \bar{w}_j^{1\ell}, \quad j = 1, 2, 3 \quad (\text{A.1a})$$

$$y_3^{1\ell} = w_3^{1\ell*} - \bar{w}_3^{1\ell} \quad (\text{A.1b})$$

where

$$w_3^{1\ell} = f(w_1^{1\ell}, w_2^{1\ell}) \left| \begin{array}{l} w_1^{1\ell} = y_1^{1\ell} + \bar{w}_1^{1\ell} \\ w_2^{1\ell} = y_2^{1\ell} + \bar{w}_1^{1\ell} \end{array} \right. \quad (\text{A.1c})$$

Since only the means were changed, the covariance remains unchanged.

By employing transformation (A.1), (3.14) can be rewritten as

$$P_e = \frac{1}{4} \sum_{\ell=1}^4 \int_{-\infty}^{\infty} \int_{-\infty}^{\infty} \int_{-\infty}^{y_3^{1\ell*}} p(Y^{1\ell}) \prod_{j=1}^3 dy_j^{1\ell} \quad (\text{A.2a})$$

where

$$p(Y^{1l}) = \frac{e^{-\frac{1}{2} Y^{1lT} \Phi_W^{-1} Y^{1l}}}{(2\pi)^{3/2} |\Phi_W|^{1/2}} \quad (\text{A.2b})$$

The quadratic form of (A.2b) can be expanded as follows

$$Y^{1lT} \Phi_W^{-1} Y^{1l} = \sum_{i=1}^3 \sum_{j=1}^3 \sigma^{ij} y_i^{1l} y_j^{1l} \quad (\text{A.3a})$$

$$= \sigma^{33} \left( y_3^{1l} + \frac{1}{\sigma^{33}} \sum_{i=1}^2 \sigma^{3i} y_i^{1l} \right)^2 + \sum_{i=1}^2 \sum_{j=1}^2 \left( \sigma^{ij} - \frac{\sigma^{3i} \sigma^{3j}}{\sigma^{33}} \right) y_i^{1l} y_j^{1l} \quad (\text{A.3b})$$

where

$$\Phi_W = [\sigma_{ij}] \quad , \quad \Phi_W^{-1} = [\sigma^{ij}] \quad (\text{A.4})$$

Now let

$$z_{1l} = y_3^{1l} + \frac{1}{\sigma^{33}} \sum_{i=1}^2 \sigma^{3i} y_i^{1l} \quad (\text{A.5a})$$

$$\bar{\sigma}^{ij} = \sigma^{ij} - \frac{\sigma^{3i} \sigma^{3j}}{\sigma^{33}} ; \quad i, j = 1, 2 \quad (\text{A.5b})$$

and

$$z_{1l}^* = y_3^{1l*} + \frac{1}{\sigma^{33}} \sum_{i=1}^2 \sigma^{3i} y_i^{1l} \quad (\text{A.6})$$

Substituting (A.5) into (A.3b) yields

$$Y^{1lT} \Phi_W^{-1} Y^{1l} = \sigma^{33} z_{1l}^2 + \sum_{i=1}^2 \sum_{j=1}^2 \bar{\sigma}^{ij} y_i^{1l} y_j^{1l} \quad (\text{A.7})$$



Now  $P_e$  can be expressed as

$$P_e = \frac{1}{4} \sum_{\ell=1}^4 \int_{-\infty}^{\infty} \int_{-\infty}^{\infty} \int_{-\infty}^{z_{1\ell}^*} \frac{e^{-\frac{1}{2} \sum_{i=1}^2 \sum_{j=1}^2 \sigma^{ij} y_i^{1\ell} y_j^{1\ell} - \frac{\sigma^{33}}{2} z_{1\ell}^2}}{(2\pi)^{3/2} |\Phi_W|^{\frac{1}{2}}} dz_{1\ell} dy_2 dy_1 \quad (A.8)$$

Consider the integration on  $z_{1\ell}$  first

$$\int_{-\infty}^{z_{1\ell}^*} e^{-\frac{1}{2} (\sqrt{\sigma^{33}} z_{1\ell})^2} dz_{1\ell} = \sqrt{\frac{2\pi}{\sigma^{33}}} \int_{-\infty}^{z_{1\ell}^*} \frac{e^{-\frac{1}{2} (\sqrt{\sigma^{33}} z_{1\ell})^2}}{\sqrt{2\pi} / \sqrt{\sigma^{33}}} dz_{1\ell} \quad (A.9)$$

Now let

$$u = \sqrt{\frac{\sigma^{33}}{2}} z_{1\ell}, \quad dz_{1\ell} = \sqrt{\frac{2}{\sigma^{33}}} du \quad (A.10)$$

then

$$\begin{aligned} & \int_{-\infty}^{z_{1\ell}^*} \frac{e^{-\left(\sqrt{\frac{\sigma^{33}}{2}} z_{1\ell}\right)^2}}{\sqrt{2\pi} / \sqrt{\sigma^{33}}} dz_{1\ell} \\ &= \frac{1}{2} - \sqrt{\frac{2}{\sigma^{33}} \cdot \frac{\sigma^{33}}{2\pi}} \int_0^{-\sqrt{\frac{\sigma^{33}}{2}} z_{1\ell}^*} e^{-u^2} du \quad (A.11a) \end{aligned}$$

$$= \frac{1}{2} \left( 1 - \frac{2}{\sqrt{\pi}} \int_0^{-\sqrt{\frac{\sigma^{33}}{2}} z_{1\ell}^*} e^{-u^2} du \right) \quad (A.11b)$$

$$= \frac{1}{2} \left[ 1 - \operatorname{erf} \left( -\sqrt{\frac{\sigma^{33}}{2}} z_{1\ell}^* \right) \right] \quad (A.11c)$$

Substituting (A.11c) into (A.9) and that result into (A.8) yields

$$P_e = \frac{1}{4} \sum_{\ell=1}^4 \int_{-\infty}^{\infty} \int_{-\infty}^{\infty} \frac{e^{-\frac{1}{2} \sum_{i=1}^2 \sum_{j=1}^2 \bar{\sigma}^{ij} y_i^{1\ell} y_j^{1\ell}}}{4\pi \sqrt{\sigma^{33}} |\Phi_W|} \cdot \left[ 1 - \operatorname{erf} \left( -\sqrt{\frac{\sigma^{33}}{2}} z_{1\ell}^* \right) \right] dy_2^{1\ell} dy_1^{1\ell} \quad (\text{A.12})$$

$y_i^{1\ell}, y_j^{1\ell}$  are dummy variables; therefore, the only dependence on the superscript  $\ell$  is in the error function argument. Dropping the superscripts on the  $y$ 's and expanding (A.12) yields

$$P_e = \frac{1}{2} \int_{-\infty}^{\infty} \int_{-\infty}^{\infty} \frac{e^{-\frac{1}{2} \sum_{i=1}^2 \sum_{j=1}^2 \bar{\sigma}^{ij} y_i y_j}}{2\pi \sqrt{\sigma^{33}} |\Phi_W|} dy_2 dy_1 - \frac{1}{8} \int_{-\infty}^{\infty} \int_{-\infty}^{\infty} \frac{e^{-\frac{1}{2} \sum_{i=1}^2 \sum_{j=1}^2 \bar{\sigma}^{ij} y_i y_j}}{2\pi \sqrt{\sigma^{33}} |\Phi_W|} \sum_{\ell=1}^4 \operatorname{erf} \left( -\sqrt{\frac{\sigma^{33}}{2}} z_{1\ell}^* \right) dy_2 dy_1 \quad (\text{A.13})$$

Mood<sup>24</sup> has shown that the first term is  $\frac{1}{2}$ ; therefore the final form for  $P_e$  is

$$P_e = \frac{1}{2} - \frac{1}{8} \int_{-\infty}^{\infty} \int_{-\infty}^{\infty} \frac{e^{-\frac{1}{2} \sum_{i=1}^2 \sum_{j=1}^2 \sigma^{ij} y_i y_j}}{2\pi \sqrt{\sigma^{33}} |\Phi_W|} \cdot \sum_{\ell=1}^4 \operatorname{erf} \left( -\sqrt{\frac{\sigma^{33}}{2}} z_{1\ell}^* \right) dy_2 dy_1 \quad (\text{A.14a})$$

where

$$z_{1\ell}^* = \ln \left[ -\frac{B}{2A} + \sqrt{\left(\frac{B}{2A}\right)^2 - \frac{C}{A}} \right] - \frac{\bar{w}_3^{\ell\ell}}{\sigma^{33}} + \frac{1}{\sigma^{33}} \sum_{i=1}^2 \sigma^{3i} y_i \quad (\text{A.14b})$$

From (3.13) and (A.1)

$$A = a_{13} + a_{14} e^{y_1 + \frac{\bar{w}_1^{\ell\ell}}{\sigma^{11}} - y_2 - \frac{\bar{w}_2^{\ell\ell}}{\sigma^{22}}} \quad (\text{A.14c})$$

$$B = a_{11} (e^{y_1 + \frac{\bar{w}_1^{\ell\ell}}{\sigma^{11}}} - e^{-y_1 - \frac{\bar{w}_1^{\ell\ell}}{\sigma^{11}}}) + a_{12} (e^{y_2 + \frac{\bar{w}_2^{\ell\ell}}{\sigma^{22}}} - e^{-y_2 - \frac{\bar{w}_2^{\ell\ell}}{\sigma^{22}}}) \quad (\text{A.14d})$$

$$C = - (a_{13} + a_{14} e^{y_2 + \frac{\bar{w}_2^{\ell\ell}}{\sigma^{22}} - y_1 - \frac{\bar{w}_1^{\ell\ell}}{\sigma^{11}}})$$

Also from (3.7) and (3.8)

$$\frac{\bar{w}_j^{\ell\ell}}{\sigma^{jj}} = \frac{1}{N_0} Z_{1\ell}^T Z_{1j} ; \quad j = 1, 2, 3 ; \quad \ell = 1, 2, 3, 4 \quad (\text{A.15a})$$

$$\frac{\bar{w}_j^{\ell\ell}}{\sigma^{jj}} = \begin{cases} \sigma^{\ell j} & ; \quad \ell, j = 1, 2, 3 \\ \sigma_{1j} - \sigma_{2j} + \sigma_{3j} & ; \quad \ell = 4 ; \quad j = 1, 2, 3 \end{cases} \quad (\text{A.15b})$$

Now from (3.4)

$$a_{1j} = \begin{cases} -\frac{1}{2} \sigma_{jj} & , \quad j = 1, 2, 3 \\ -\frac{1}{2} [\sigma_{11} + \sigma_{22} + \sigma_{33} + 2(\sigma_{13} - \sigma_{12} - \sigma_{23})] & , \quad j = 4 \end{cases} \quad (A.16)$$

The covariance of  $w_i^{kl}$  and  $w_j^{kl}$  is not a function of  $k$  or  $l$  and is obtained by substituting (3.5) into (3.7) and evaluating for the covariance. The elements of  $\Phi_W$  are

$$\sigma_{11} = 2 \frac{E_0}{N_0} (1 + 2\rho) \quad (A.17a)$$

$$\sigma_{12} = 2 \frac{E_0}{N_0} (1 - a + \rho) \quad (A.17b)$$

$$\sigma_{13} = 0 \quad (A.17c)$$

$$\sigma_{22} = 2 \frac{E_0}{N_0} \quad (A.17d)$$

$$\sigma_{23} = 2 \frac{E_0}{N_0} (a - \rho) \quad (A.17e)$$

$$\sigma_{33} = 2 \frac{E_0}{N_0} (1 - 2\rho) \quad (A.17f)$$

and of course

$$\sigma_{ij} = \sigma_{ji} \quad ; \quad i, j = 1, 2, 3 \quad (A.17g)$$

where  $E_0$  is defined by (4.26),  $\rho$  is defined by (4.29) and the normalized head energy -  $a$  is defined by

$$a = \frac{\int_{-L}^L z^2(t) dt}{E_0} \quad (A.18)$$

$E_o/N_o$  is defined as "signal-to-noise" ratio, where  $N_o$  is the noise variance.

Equation (A.14a) was numerically integrated<sup>22</sup> to determine the performance of the Bayes receiver for adjacent baud overlap and equiprobable, bipolar signals. The performance curves are given in Figure 3-1.

From (A.15), (A.16) and (A.17),  $P_e$  can be expressed as a function of only three parameters, i.e.,

$$P_e = f(E_o/N_o, \rho, a) \quad (A.19)$$

## APPENDIX B

This appendix discusses a numerical method used to solve the Fredholm equation of the second kind in (4.20b) for the maximum eigenvalue and corresponding optimum signal. This method was developed for an arbitrary kernel and hence for an arbitrary channel. It was successfully computer implemented<sup>23</sup>. The integral was numerically integrated by a rectangular integration rule. A rectangular rule was chosen in order to preserve symmetry. Then  $n$  points in time were chosen to form a system<sup>18</sup> of  $n$  equations. These  $n$  equations were solved for the maximum eigenvalue and corresponding eigenvector by an iterative technique<sup>21</sup>.

By employing a rectangular integration rule (4.20b) can be expressed in a limiting form as

$$\lim_{n \rightarrow \infty} d \sum_{j=1}^n K(t, \tau_j) s(\tau_j) = \lambda_1 s(t), \quad -L \leq t, \tau \leq L \quad (\text{B.1})$$

where

$$d = |\tau_{j+1} - \tau_j|$$

Then for a particular instant of time  $t = t_i$

$$d \sum_{j=1}^n K(t_i, \tau_j) s(\tau_j) \doteq \lambda_1 s(t_i) \quad (\text{B.2})$$

Let

$$s_i = s(t_i) \quad (\text{B.3a})$$

$$s_j = s(\tau_j) \quad (\text{B.3b})$$

$$k_{ij} = K(t_i, \tau_j) \quad (\text{B.3c})$$

For convenience, the approximate sign in (B.2) will be dropped. Now a linear system of  $n$  equations can be formed by selecting  $n$  points in time, i.e.,

$$\left. \begin{aligned} d \sum_{j=1}^n k_{1j} s_j &= \lambda_1 s_1 \\ d \sum_{j=1}^n k_{2j} s_j &= \lambda_1 s_2 \\ &\vdots \\ d \sum_{j=1}^n k_{nj} s_j &= \lambda_1 s_n \end{aligned} \right\} \quad (\text{B.4})$$

In matrix form (B.4) becomes

$$d K S = \lambda_1 S \quad (\text{B.5})$$

yielding a discrete eigenvalue problem with symmetric kernel.

The iterative scheme<sup>21</sup> presented here to compute the maximum eigenvalue and corresponding eigenvector can best be described by the following outline

1. Choose initial vector

$$S^{(0)} = \begin{bmatrix} 1 \\ 1 \\ \vdots \\ 1 \end{bmatrix} \quad (\text{B.6})$$

2. Try initial vector as a solution in (B.5); multiply out

$$d K S^{(0)} = X^{(1)} \quad (\text{B.7})$$

3. Normalize  $X^{(1)}$  to first component and set

$$S^{(1)} = \frac{X^{(1)}}{x_1^{(1)}} \quad (\text{B.8a})$$

$$\lambda_1 = x_1^{(1)} \quad (\text{B.8b})$$

4. Try  $S^{(1)}$  as a solution, multiply out

$$d K S^{(1)} = X^{(2)} \quad (\text{B.9})$$

5. Normalize

$$S^{(2)} = \frac{X^{(2)}}{x_1^{(2)}} \quad (\text{B.10a})$$

$$\lambda_1^{(2)} = x_1^{(2)} \quad (\text{B.10b})$$

6. Iterate procedure k times until desired accuracy is obtained.

7. Then

$$S \doteq \frac{X^{(k)}}{x_1^{(k)}} \quad (\text{B.11a})$$

$$\lambda_1 \doteq x_1^{(k)} \quad (\text{B.11b})$$

In the cases studied in this research the maximum eigenvalue converged to within 10 per cent accuracy in the third significant digit with no more than 20 iterations. For example, an eigenvalue of 0.500 in the kth iteration was greater than 0.499 on the k-1 iteration. Since (B.4) represents n equations with n+1 unknowns, the solution in (5.11a) is only determined to within an arbitrary multiplicative constant.

After the kernel is obtained by integrations on the impulse response, the number of samples,  $n \times n$ , required to represent the kernel were not excessive. For example, the RC channel kernel in section 4.4 can be solved for the approximate optimum signal using only 11 samples on  $[-L, L]$  for  $L = 0.5$  milliseconds. For practical purposes, the results did not change significantly by increasing the number of samples.



**RECENT RESEARCH PUBLICATIONS  
SCHOOL OF ELECTRICAL ENGINEERING  
PURDUE UNIVERSITY**

- TR-EE65-1 PERFORMANCE OF EASILY IMPLEMENTED ERROR REDUCTION TECHNIQUES**  
J. C. Hancock and R. G. Marquart, Contract No. AF 33(657)-10709; PRF 3474-61-780, January 1965.
- TR-EE65-2 UNSUPERVISED LEARNING RECEIVERS FOR BINARY CHANNELS WITH INTERSYMBOL INTERFERENCE.**  
J. C. Hancock and R. W. Chang. Contract No. NSF-GP-2898; PRF 3955-50-285, January 1965.
- TR-EE65-3 INVESTIGATION OF OPTIMIZATION OF ATTITUDE CONTROL SYSTEMS, VOL. I.**  
R. Sridhar, G. C. Agarwal, R. M. Burns, D. M. Detchmendi, E. H. Kopf, Jr., and R. Mukundan. Contract No. JPL-950670/SUBNAS 7-100, PRF No. 3807-55-285, January 1965.
- TR-EE65G4 INVESTIGATION OF OPTIMIZATION OF ATTITUDE CONTROL SYSTEMS, VOL. II.**  
R. Sridhar, G. C. Agarwal, R. M. Burns, D. M. Detchmendi, E. H. Kopf, Jr., and R. Mukundan. Contract No. JPL-950670/SUBNAS 7-100, PRF No. 3807-55-285, January 1965.
- TR-EE65-5 SOLID STATE MICROWAVE POWER RECTIFIERS.**  
R. H. George. Contract No. AF30(602)3481, PRF No. 411-53-285, February 1965.
- TR-EE65-6 SEQUENTIAL DECISIONS, PATTERN RECOGNITION AND MACHINE LEARNING.**  
K. S. Fu and C. H. Chen. Contract No. NSF G-2183, PRF 3810, PRF 3373 - David Ross Grant, April 1965.
- TR-EE65-7 PRESSURE SENSITIVITY OF ALLOYED P-N JUNCTIONS**  
H. W. Thompson, Jr. Contract No. N123(953)35011A, PRF 3832-53-2859. June 1965.
- TR-EE65-8 A STUDY OF STOCHASTIC AUTOMATA AS MODELS OF ADAPTIVE AND LEARNING CONTROLLERS.**  
K. S. Fu and G. T. McMurtry. Contract No. NSF G-2183; PRF 3810; June 1965.
- TR-EE65-9 SPEECH ANALYSIS.**  
G. W. Hughes and J. F. Hemdel. Contract No. AF19(628)-305 with Air Force Cambridge Research Labs., Bedford, Massachusetts; PRF 3080-53-285.
- TR-EE65-10 ADVANCED CONTROL TECHNIQUES APPLIED TO LARGE FLEXIBLE LAUNCH VEHICLES VOLUME I.**  
J. E. Gibson, V. Haas, J. C. Hill, L. E. Jones, A. S. Morse, S. Murtuza, A. M. Steinberg. Contract No. NASA 8-11416; NASAMSFC, Huntsville, Alabama; PRF 4005-52-285.
- TR-EE65-11 ADVANCED CONTROL TECHNIQUES APPLIED TO LARGE FLEXIBLE LAUNCH VEHICLES VOLUME II.**  
J. E. Gibson, V. Haas, J. C. Hill, L. E. Jones, A. S. Morse, S. Murtuza, A. M. Steinberg. Contract No. NASA 8-11416; NASAMSFC, Huntsville, Alabama; PRF 4005-52-285. July 1965.
- TR-EE65-12 ADAPTIVE AND LEARNING CONTROL SYSTEMS-FINAL REPORT.**  
J. E. Gibson and K. S. Fu. Contract No. AF AFOSR 62-531; Air Force Office of Scientific Research; PRF 3123-57-285; July 1965.
- TR-EE65-13 ANALYSIS AND DESIGN OF NONLINEAR CONTROL SYSTEMS-FINAL REPORT.**  
J. E. Gibson, Principal Investigator; J. B. Pearson, Principal Investigator; Authors-J. B. Pearson, J. R. Rowland, G. N. Saridis, and P. H. Swain. Contract No. AF 29(600)-3566, Air Force Missile Development Center, Holloman Air Force Base; PRF 3304; August 1965.
- TR-EE65-14 AN ADAPTIVE PATTERN RECOGNITION MACHINE USING NEURON-LIKE ELEMENTS.**  
K. S. Fu and W. C. Lin. Contract No. NSF Grant GP-2183; PRF 3810-50-285; August 1965.
- TR-EE65-15 ESTIMATION OF PROBABILITY DENSITY AND DISTRIBUTION FUNCTIONS.**  
G. R. Cooper and J. A. Tabaczynski. Contract No. NSF Grant G-18997; PRF 2974; August 1965.
- TR-EE65-16 LOWER BOUNDS ON THE THRESHOLDS OF SUBHARMONIC OSCILLATIONS.**  
D. R. Anderson and T. N. Trick. Contract No. National Science Foundation Grant GK26; PRF 4108, September 1965.
- TR-EE65-17 AN APPLICATION OF STOCHASTIC AUTOMATA TO THE SYNTHESIS OF LEARNING SYSTEMS.**  
K. S. Fu and R. W. McLaren. Contract No. National Science Foundation Grant GP-2183; PRF 3810, September, 1965.
- TR-EE65-18 A UNIFIED N-PORT SYSTEM THEORY**  
L. O. Chua and B. J. Leon, National Science Foundation Grant GK-26, PRF 4180, September, 1965.
- TR-EE65-19 ON RECEPTION OF SIGNALS FOR CHANNELS HAVING MEMORY**  
J. C. Hancock and R. W-L. Chang, National Science Foundation Grant GP-2898, PRF 3955, October, 1965.

**RECENT RESEARCH PUBLICATIONS  
SCHOOL OF ELECTRICAL ENGINEERING  
PURDUE UNIVERSITY**

- TR-EE65-20 LEARNING THEORY APPLIED TO COMMUNICATIONS**  
Dwight F. Mix and John C. Lindenlaub, Air Force Contract AF33(615)-2620, PRF #4218-53-285, October, 1965
- TR-EE65-21 LEARNING PROBABILITY SPACES FOR CLASSIFICATION AND RECOGNITION OF PATTERNS WITH OR WITHOUT SUPERVISION**  
E. A. Patrick and J. C. Hancock, National Aeronautics and Space Administration Contract NsG-553 PRF #3823-52-285, November, 1965
- TR-EE66-1 TOWARD BRAIN MODELS WHICH EXPLAIN MENTAL CAPABILITIES - (Report No. 1)**  
R. J. Swallow, Support: E. E. Department Research
- TR-EE66-2 ON THE ASYMPTOTIC STABILITY OF FEEDBACK CONTROL SYSTEMS CONTAINING A SINGLE TIME-VARYING ELEMENT**  
Z. V. Rekasius and J. R. Rowland, NASA Institutional Grant (SUB-UNDER NRG 14-005-021) PRF #4220-52-285, January, 1966
- TR-EE66-3 ANALOGUE DEMODULATION ON A FINITE TIME INTERVAL**  
J. C. Hancock and P. W. Brunner, NSF Grant #GP-2898, PRF #3955-50-285, April, 1966
- TR-EE66-4 STEADY STATE ANALYSIS OF LINEAR NETWORKS CONTAINING A SINGLE SINUSOIDALLY VARYING ELEMENT.**  
B. J. Leon and J. V. Adams, Grant #GK26, PRF #4108-50-285, May, 1966
- TR-EE66-5 CYBERNETIC PREDICTING DEVICES**  
A. G. Ivakhnenko and V. G. Lapa. Translated by Z. J. Nikolic, April, 1966
- TR-EE66-6 ON THE STOCHASTIC APPROXIMATION AND RELATED LEARNING TECHNIQUES**  
K. S. Fu, Y. T. Chien, Z. J. Nikolic and W. G. Wee, National Science Foundation GK-696, PRF #4502, April, 1966